JOC The Journal of Organic Chemistry

Article

pubs.acs.org/joc

Regioselective Oxidation of Nonactivated Alkyl C−H Groups Using Highly Structured Non-Heme Iron Catalysts

Laura Gómez,[†] Mercè Canta,[†] David Font, Irene Prat, Xavi Ribas, and Miquel Costas*

QBIS Research Group, Departament de Química, Universitat de Girona, Campus Montilivi, Girona E-17071, Catalonia, Spain

Supporting Information

ABSTRACT: Selective oxidation of alkyl C−H groups constitutes one of the highest challenges in organic synthesis. In this work, we show that mononuclear iron coordination complexes Λ-[Fe(CF_3SO_3)$_2$((*S*,*S*,*R*)-MCPP)] (**Λ-1P**), Δ-[Fe(CF_3SO_3)$_2$((*R*,*R*,*R*)-MCPP)] (**Δ-1P**), Λ-[Fe(CF_3SO_3)$_2$((*S*,*S*,*R*)-BPBPP)] (**Λ-2P**), and Δ-[Fe(CF_3SO_3)$_2$((*R*,*R*,*R*)-BPBPP)] (**Δ-2P**) catalyze the fast, efficient, and selective oxidation of nonactivated alkyl C−H groups employing H_2O_2 as terminal oxidant. These complexes are based on tetradentate N-based ligands and contain iron centers embedded in highly structured coordination sites defined by two bulky 4,5-pinenopyridine donor ligands, a chiral diamine ligand backbone, and chirality at the metal (Λ or Δ). X-ray diffraction analysis shows that in **Λ-1P** and **Λ-2P** the pinene rings create cavity-like structures that isolate the iron site. The efficiency and regioselectivity in catalytic C−H oxidation reactions of these structurally rich complexes has been compared with those of Λ-[Fe(CF_3SO_3)$_2$((*S*,*S*)-MCP)] (**Λ-1**), Λ-[Fe(CF_3SO_3)$_2$((*S*,*S*)-BPBP)] (**Λ-2**), Δ-[Fe(CF_3SO_3)$_2$((*R*,*R*)-BPBP)] (**Δ-2**), Λ-[Fe(CH_3CN)$_2$((*S*,*S*)-BPBP)](SbF_6)$_2$ (**Λ-2SbF$_6$**), and Δ-[Fe(CH_3CN)$_2$((*R*,*R*)-BPBP)](SbF_6)$_2$ (**Δ-2SbF$_6$**), which lack the steric bulk introduced by the pinene rings. Cavity-containing complexes **Λ-1P** and **Λ-2P** exhibit enhanced activity in comparison with **Δ-1P**, **Δ-2P**, **Λ-1**, **Λ-2**, and **Λ-2SbF$_6$**. The regioselectivity exhibited by catalysts **Λ-1P**, **Λ-2P**, **Δ-1P**, and **Δ-2P** in the C−H oxidation of simple organic molecules can be predicted on the basis of the innate properties of the distinct C−H groups of the substrate. However, in specific complex organic molecules where oxidation of multiple C−H sites is competitive, the highly elaborate structure of the catalysts allows modulation of C−H regioselectivity between the oxidation of tertiary and secondary C−H groups and also among multiple methylene sites, providing oxidation products in synthetically valuable yields. These selectivities complement those accomplished with structurally simpler oxidants, including non-heme iron catalysts **Λ-2** and **Λ-2SbF$_6$**.

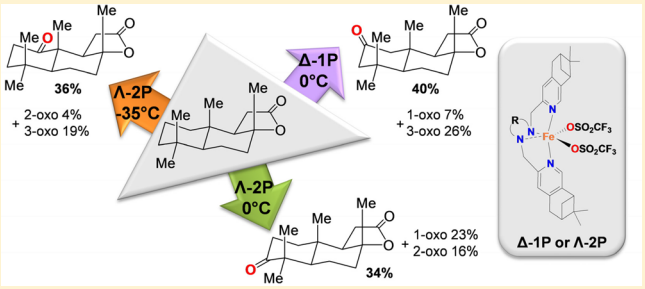

INTRODUCTION

Oxidized hydrocarbons constitute a basic structural motif in organic molecules. Prominent examples constitute families of natural products such as terpenes[1,2] and steroids,[3] and particularly interesting are molecules of pharmacological relevance such as artemisin,[4] taxanes,[5] and briostatin,[6] to name a few representative examples. Therefore, one of the most attractive strategies in organic synthesis is the development of methodologies that allow for the site-selective oxidation of alkyl sp^3 C−H groups.[7−14] The factors that govern regioselectivity in these reactions have been actively pursued and identified.[7] Electronic effects have an impact on the strength of the C−H bond, and in the absence of directing groups, they most commonly dominate selectivity. This is so because most reagents that can engage in C−H oxidation reactions have simple architectures and also do not participate in organometallic interactions.[15−20] Consequently, in most cases structural constraints imposed by the oxidant are not important. In addition, most oxidizing agents are limited in scope to tertiary C−H groups and activated methylene sites, and very few examples of oxidants exist that can also efficiently and selectively oxidize stronger C−H groups in addition to simple cycloalkanes.[21−26] Discovery of reagents that could bias this general reactivity are particularly valuable, because they will complement current methodologies and open novel synthetic paths.

The most successful strategy to divert C−H regioselectivity in C−H oxidations is the use of directing groups, either of covalent nature[27−31] or based in metal-coordination bonds.[28,32−36] A more subtle and elaborated approach exploited by enzymes relies on employing highly spatially structured oxidizing sites that could regulate selectivity by controlling access and orientation of the substrate in its approach toward the oxidizing unit. The design of bioinspired iron catalysts is envisioned as a promising tool to pursue this strategy.[37−41] Fe-based catalytic methods are also particularly appealing, due to the availability and the lack of toxicity of this element and because iron-based reagents are very reactive and can hydroxylate not only 3° C−H groups but also 2° alkyl sites, thus complementing existing oxidizing methodologies.[42−55] Despite the potential of this approach, few iron-based systems provide C−H oxidized products with synthetically amenable

Received: October 26, 2012
Published: January 10, 2013

dx.doi.org/10.1021/jo302196q | *J. Org. Chem.* 2013, 78, 1421−1433

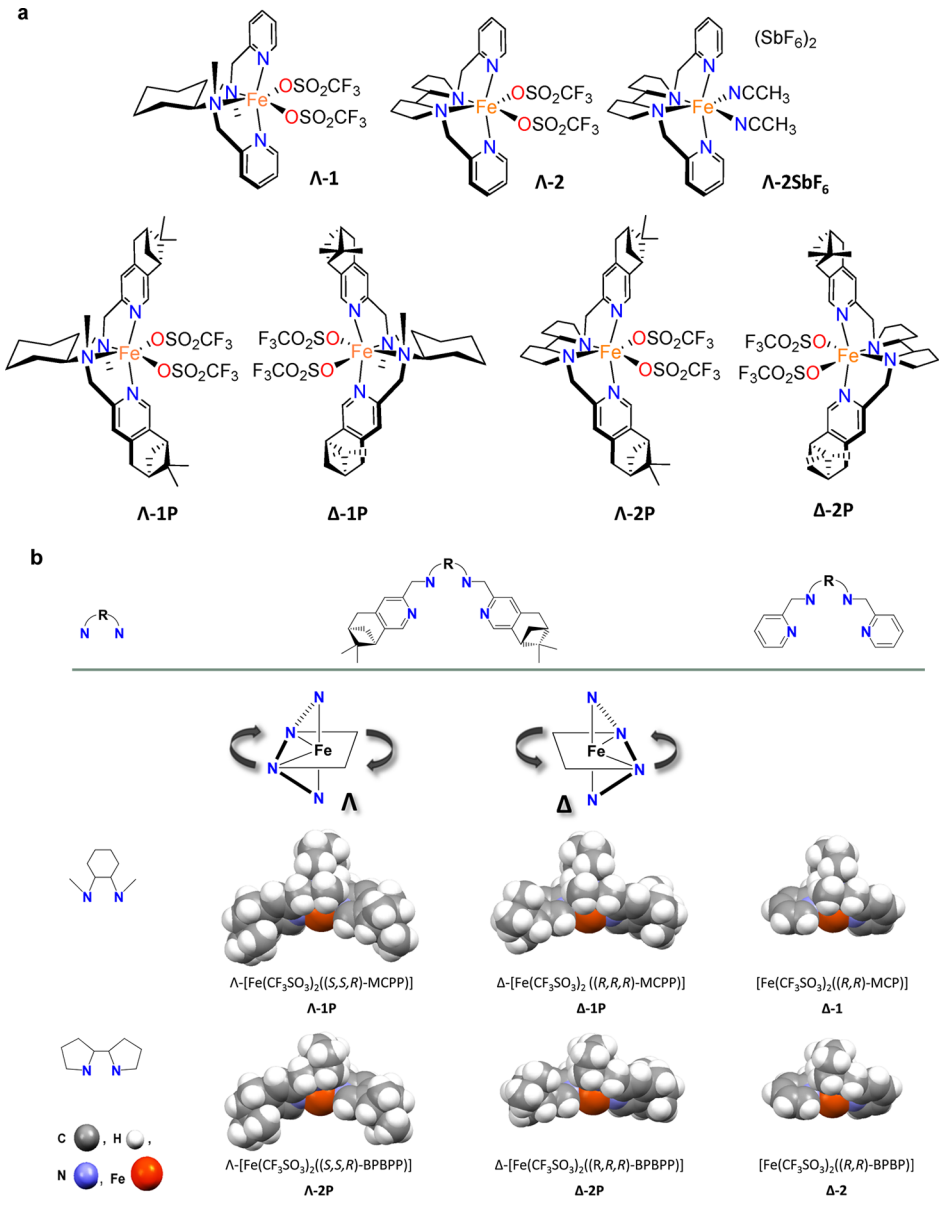

Figure 1. Catalyst structure: (a) 3D chemical diagrams of **Λ-1**, **Λ-2**, **Λ-2SbF$_6$**, **Λ-1P**, **Δ-1P**, **Λ-2P**, and **Δ-2P**; (b) space-filling diagrams of **Λ-1P**, **Δ-1P**, **Λ-2P**, **Δ-2P**, Δ-[Fe(CF$_3$SO$_3$)$_2$((*R*,*R*)-MCP)] (**Δ-1**)[57] and **Δ-2**.[58] Counterions and solvent of crystallization have been omitted for clarity. Details on the experimental parameters of the X-ray diffraction analysis and tables with bond distances and angles are given in the Supporting Information.

yields, albeit with modest turnover numbers and C−H regioselectivities.

We have recently shown that a highly active non-heme iron catalyst for the selective oxidation of alkyl C−H groups with H_2O_2 is obtained by introducing steric bulk at the catalyst active site, creating a robust, well-defined cavity.[51] Herein, we show that this family of structurally elaborated catalysts imparts alternative or improved C−H site selectivities that escape from the inherent reactivity of C−H bonds, without the aid of directing groups. In addition to the steric hindrance, the chirality of the catalysts and the nature of the ligand diamine backbone are identified as additional key structural aspects of the iron catalyst active site that have an impact on C−H site selectivity. These selectivities complement those accomplished with structurally simpler oxidants, including non-heme catalysts described to date.

RESULTS AND DISCUSSION

Mononuclear iron complexes Λ-[Fe(CF$_3$SO$_3$)$_2$((*S*,*S*,*R*)-MCPP)] (**Λ-1P**), Δ-[Fe(CF$_3$SO$_3$)$_2$((*R*,*R*,*R*)-MCPP)] (**Δ-1P**), Λ-[Fe(CF$_3$SO$_3$)$_2$((*S*,*S*,*R*)-BPBPP)] (**Λ-2P**), and Δ-[Fe(CF$_3$SO$_3$)$_2$((*R*,*R*,*R*)-BPBPP)] (**Δ-2P**) (Figure 1; Δ and Λ indicate the chirality at the metal and the P after the number indicates that the ligand contains pinene rings fused to 4,5-positions of the pyridine) where prepared by using the two pairs of ligands (*S*,*S*,*R*)-MCPP, (*R*,*R*,*R*)-MCPP and (*S*,*S*,*R*)-BPBPP, (*R*,*R*,*R*)-BPBPP, differing in the nature and chirality of the aliphatic diamine backbone.

Complexes **Λ-1P**, **Δ-1P**, **Λ-2P**, and **Δ-2P** present chirality at the metal, which in turn is determined by the chirality of the diamine backbone.[56] (*S*,*S*)- and (*R*,*R*)-diamines predetermine generation of complexes with Λ and Δ chirality at the metal, respectively. The combination of the chirality of the aliphatic

dx.doi.org/10.1021/jo302196q | J. Org. Chem. 2013, 78, 1421−1433

diamine (*S*,*S* or *R*,*R*) with that of the (+)-pinene group allows control over the relative orientation of the methyl groups of the pinene with respect to the *cis*-exchangeable sites at the iron center. This structural feature provides a certain degree of control over the space around the metal site, where the oxidant presumably binds and substrate oxidation takes place. The space-filling analysis (Figure 1b) shows that in **Λ-1P** and **Λ-2P** the iron site is surrounded by a well-defined cavity-like space. Instead, in all other complexes, the two exchangeable *cis* coordination sites are exposed to the bulk. ^{1}H NMR analyses indicate that the C_2-symmetric structure of the solid state is retained in solution. We envisioned that the differential spatial structures of the complexes, and especially the chirality at the metal and the cavity-like architecture of **Λ-1P** and **Λ-2P** surrounding iron labile sites will have an impact on the selectivity of the catalysts in C−H oxidation reactions by regulating access of the substrate to the active site on the basis of its size, chirality, and shape.

Catalyst Stability. In order to test the influence of the pinene group and the nature of the diamine backbone on the oxidation activity of these catalysts in C−H oxidation reactions, a time profile of product formation in the oxidation of (−)-menthyl acetate (**3**) with H_2O_2 mediated by **Λ-1P**, **Δ-1P**, **Λ-2P**, and **Δ-2P** and the structurally simpler catalysts Λ-[Fe(CF$_3$SO$_3$)$_2$((*S*,*S*)-MCP)] (**Λ-1**), Λ-[Fe(CF$_3$SO$_3$)$_2$((*S*,*S*)-BPBP)] (**Λ-2**), and Λ-[Fe(CH$_3$CN)$_2$((*S*,*S*)-BPBP)](SbF$_6$)$_2$ (**Λ-2SbF$_6$**) (1 mol %) was monitored (Figure 2a; see Figure 1

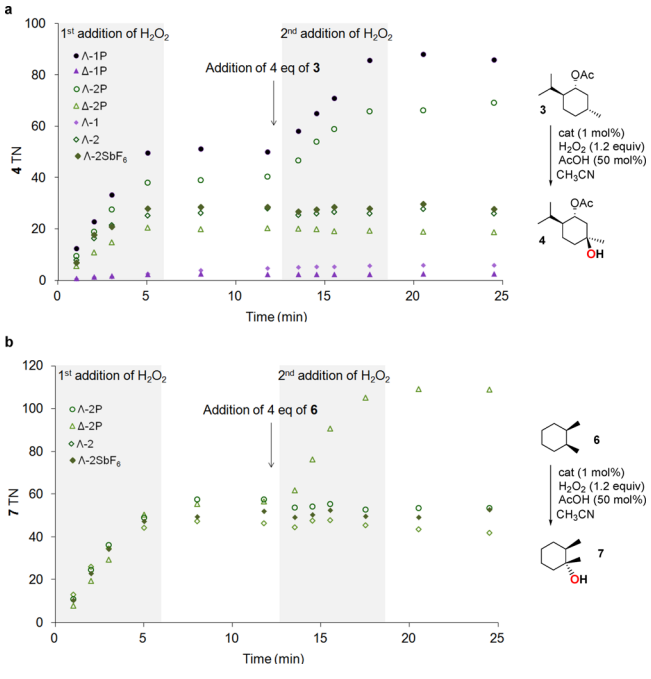

Figure 2. Catalyst stability: (a) oxidation of (−)-menthyl acetate (**3**) (formation of **4** in the hydroxylation of **3** represented versus time in two-step addition of H_2O_2 in presence of large excess of substrate); (b) oxidation of *cis*-1,2-dimethylcyclohexane (**6**) (formation of **7** in the hydroxylation of **6** represented versus time in two-step addition of H_2O_2 in the presence of a large excess of substrate).

for catalyst structures). Irrespective of the catalyst, oxidation of **3** produces tertiary alcohol **4** with high selectivity (77−90% selectivity depending on the catalyst; see Figure 4b). Reactions were fast and were finished immediately after H_2O_2 addition was complete. The structure of the aliphatic diamine plays a crucial role in the efficiency of the reactions. Complex **Λ-1**, with a cyclohexanediamine backbone,[59] is less efficient than the bipyrrolidine-based complex **Λ-2**.[58] The introduction of the pinene ring in complexes with Δ topology does not have much of an influence on the outcome efficiency of the catalysts (compare **Λ-1** vs **Δ-1P** and **Λ-2** vs **Δ-2P**). On the other hand, Λ complexes containing pinene groups (**Λ-1P** and **Λ-2P**) exhibit substantially better efficiency than the analogous **Λ-1** and **Λ-2**, which lack this group. Moreover, the presence of a well-defined ligand cavity around the iron ion in complexes **Λ-1P** and **Λ-2P** increases the stability of the catalyst resting state, since only these complexes maintain their activity after the first H_2O_2 addition. Indeed, for the particular case of **Λ-1P**, the number of turnovers (TN) of alcohol product **4** obtained in the first and second H_2O_2 additions are comparable (50 and 45 TN, respectively; **Λ-2P** provides 39 and 28 TN, respectively). Finally, the activity of **Λ-2** and **Λ-2SbF$_6$** appear to be nearly identical, suggesting that triflate and SbF_6 anions have no influence on the relative activities of the two catalysts. The conclusions arising from the time profile analysis of the oxidation of (−)-menthyl acetate (**3**) were further confirmed by performing analogous experiments in the oxidation of *cis*-1,2-dimethylcyclohexane (**6**) (see Figure 2b).

These observations thus demonstrate that both the presence of the pinene rings and the proper combination of the chirality at the metal (Λ/Δ), with the chirality of the pinene rings, exert a profound influence on the efficiency and stability of the catalysts. Specifically, the presence of a well-defined ligand cavity around the iron ion in complexes **Λ-1P** and **Λ-2P** increases their robustness, most likely by providing protection against bimolecular deactivation pathways leading to the formation of catalytically inactive oxo-bridged ferric oligomeric species.[51]

Factors Governing Selectivity in C−H Oxidation Reactions of Simple Substrates. Complexes **Λ-1P**, **Δ-1P**, **Λ-2P**, **Δ-2P**, **Λ-1**, and **Λ-2**, were compared as catalysts in the oxidation of tertiary and secondary C−H groups (Table 1, entries 1 and 3; Table S3 Supporting Information, entries 1 and 2). The standard oxidation protocol employed consisted in a single syringe pump addition of H_2O_2 over a CH_3CN solution containing the catalyst (3 mol %), AcOH (1.5 equiv) and substrate at 0 °C. This higher level of starting catalyst loading with regard to Figure 2 and to our previous procedure[51] suffices to obtain moderate to good product yields for all catalysts using a very simple protocol (Table 1 and Table S3, Supporting Information). Interestingly, yields attained with the pinene-containing catalysts are substantially higher (up to 65% for **9** and 75% for **11**) than those obtained with their respective analogues lacking the pinene ring (**Λ-1** and **Λ-2**).

Despite being traditionally considered as inert, it is now recognized that alkyl C−H groups have distinct inherent relative reactivity in C−H functionalization reactions.[7] Selectivity patterns exhibited by this family of catalysts were studied (Table 1; reaction patterns observed for **Δ-2P** and **Λ-2** in these simple substrates are very close to those obtained for **Λ-2P**, and therefore, they are only shown in the Supporting Information).

In general 3° C−H groups are preferentially oxidized in the presence of statistically more important 2° C−H sites (Table 1, entries 1, 2, and 4−6). These reactions take place with

dx.doi.org/10.1021/jo302196q | J. Org. Chem. 2013, 78, 1421−1433

Table 1. Oxidation of Alkyl C−H Groups of Simple Alkanes[a]

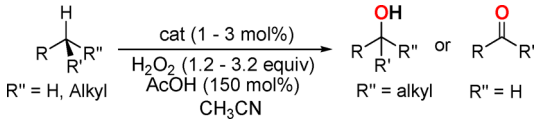

Entry	Substrate	Oxidation products				
	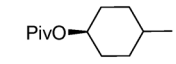	 3°OH	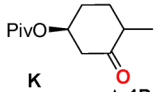 K	Yield%[b] [3°OH[c]/K][d] Λ-1P	Δ-1P	Λ-2P
1	***cis*-, 9**	**10**	**-**	51	53	65
2	***trans*-, 13**	**14**	**15**	60 [71/29]	58 [69/31]	61[80/20]
3	**cyclohexane, 11**	**cyclohexanone, 12**		72	75	71
	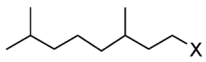	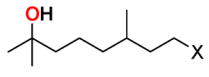 Remote	Yield%[b] [Remote/Proximal][d] Λ-1P	Δ-1P	Λ-2P	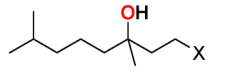 Proximal
4	**X=H, 16**	**17**	32 [55/45]	31 [55/45]	31 [48/52]	**18**
5	**X=Br, 19**	**20**	48 [88/12]	41 [90/10]	43 [85/15]	**21**
6	**X= OAc, 22**	**23**	49 [79/21]	44 [81/19]	44 [77/23]	**24**
	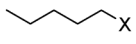	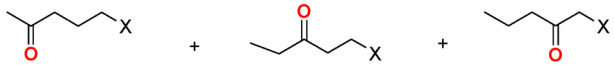 K2	Yield%[b] [K2/K3/K4][d] Λ-1P	Δ-1P	K3	Yield%[b] [K2/K3/K4][d] Λ-2P	K4
7	**X=CH_3, 25**	**26**	50 [57/43]	46 [59/41]	**27**	51 [50/50]	-
8	**X=CH_2CH_3, 28**	**29**	57 [51/35/14]	53 [47/36/17]	**30**	56 [42/40/18]	**31**
9	**X=$(CO)OCH_3$, 32**	**33**	55 [76/24]	26 [74/26]	**34**	56 [63/37]	-
10	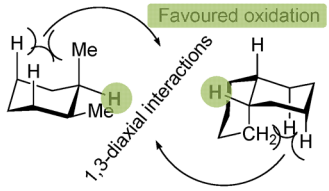 **6**	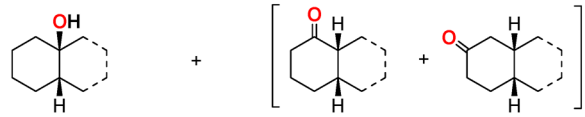 3°OH	Yield%[e] [3°OH[f]/K][d] Λ-1P	Δ-1P	Λ-2P	K
11	**35**	**36**	46 [69/31]	51 [71/29]	48 [77/23]	**37**
	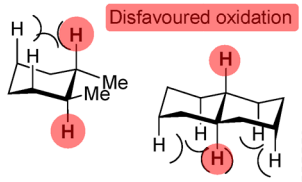 **38**	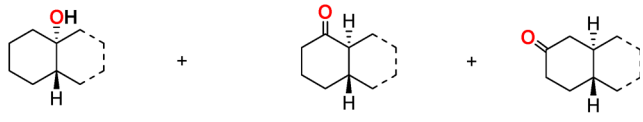 3°OH	Yield%[e] [3°OH[f]/K2/K3][d] Λ-1P	Δ-1P	K2	Yield%[e] [3°OH[f]/K2/K3][d] Λ-2P	K3
12		**39**	47 [26/29/45]	52 [28/26/46]	**40**	49 [48/24/28]	**41**
13	**42**	**43**	47 [4/37/59]	50 [7/37/56]	**44**	48 [13/40/46]	**45**
14	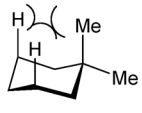 **46**	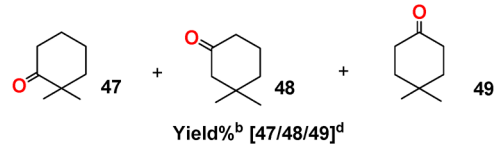 **47** **48** **49** Yield%[b] [47/48/49][d] Λ-1P	Δ-1P	Λ-2P			
		67 [23/54/23]	66 [21/57/22]	68 [37/44/19]			

[a]1,3-Diaxial interactions in *cis*- and *trans*-cyclohexane derivatives are highlighted in the corresponding chemical diagrams. See Table 2 for specific reaction conditions. [b]GC yield based on substrate (average of at least two experiments). [c]RC > 95%. [d]Normalized (100) ratio of products [e]GC yield based on substrate (average of at least three experiments). [f]RC > 98%.

stereoretention (retention of configuration (RC) > 95%). This is indicative of a metal-centered transformation where long-lived carbon-centered radicals are not involved.[45,48]

Ketones are the main products obtained in the oxidation of methylene sites (Table 1, entries 3, 7−9, and 14), presumably via a two-step oxidation of the C−H group into the

dx.doi.org/10.1021/jo302196q | J. Org. Chem. 2013, 78, 1421−1433

corresponding alcohol, which is rapidly further oxidized to the corresponding ketone. Consistent with this scenario, submitting cyclohexanol to the standard reaction conditions using **Λ-1P** as catalyst provides quantitative conversion into cyclohexanone. We also considered the possibility that hydroperoxides could be formed as reaction products,[60−62] but treating reaction mixtures with PPh_3, according to the method developed by Shul'pin,[63] did not yield enhanced amounts of alcohol products at the expense of measured ketone yields (Table S13 (Supporting Information)), discarding this possibility.

Electronic effects in the regioselective oxidation of 3° (Table 1, entries 5 and 6) and 2° C−H groups (Table 1, entry 9) showed the characteristic pattern of an electrophilically active species, preferentially oxidizing remote, more electron rich C−H sites.

Cyclohexanes constitute common basic frameworks in organic molecules and may be regarded as informative substrate probes. When they are subjected to the standard oxidation procedure, cyclohexane derivatives provide moderate to good product yields (43−75%; Tables 1, entries 1, 2 and 10−14, and Tables S3 and S6−S8 (Supporting Information)).

In cyclohexane derivatives the orientation of the C−H group to be oxidized is determinant for the regioselective outcome of the oxidation reaction.[64] Tertiary C−H groups in equatorial positions are more prone to oxidation, because they are spatially more accessible and because a strain release of the 1,3-diaxial interactions occurs in the rate-determining C−H bond-breaking step. Instead, breakage of tertiary C−H bonds in axial positions is not facilitated by strain release, and competitive oxidation between 3° and 2° sites can occur, because the latter are also spatially more accessible.

As predicted from this analysis, in substrates where at least one tertiary C−H is in an equatorial disposition (e.g., **6**, **9**, and **35**), the corresponding tertiary alcohol (**7**, **10**, and **36**, respectively), is obtained with high selectivity, good yield (up to 65%), and high retention of configuration (>95%). Instead, oxidation of the corresponding *trans* isomers (compare **6** vs **38**, **35** vs **42**, and **9** vs **13**; Table 1 and Tables S3, S6, and S7 (Supporting Information)) favor oxidation at 2° C−H sites in comparison to *cis* isomers.

In *cis* and *trans* isomers the regioselectivity toward the tertiary C−H is also influenced by steric constraint around this bond. For example, the bicyclic nature of decalins (**35** and **42**) accounts for a more efficient shielding of the tertiary C−H bond than in single cyclohexane rings, which translates in an increased preference for the oxidation of the 2° sites (compare **35** vs **6** and **9**; or **42** vs **13** and **38**, respectively). Most interestingly, however, selectivity also depends on the structure of the catalysts. The best selectivities toward oxidation of methylene sites are attained when using catalysts **Λ-1P** and **Δ-1P**, and this selectivity is remarkably acute in the oxidation of *trans*-decalin (**42**; 96% and 93%, respectively). To the best of our knowledge, such a level of selectivity has only been previously documented for Mizuno's polyoxometalates.[24]

Moreover, catalysts **Λ-1P** and **Δ-1P** exhibit remarkable discrimination between methylene position 2 (ketone K2 formed) and position 3 (K3 formed), in favor of the latter, which is the least sterically hindered (Table 1, entries 12 and 13). Instead, catalysts **Λ-2P**, **Δ-2P**, and **Λ-2** (Table S7 (Supporting Information)) show almost no discrimination between the two methylene sites. This is also observed in the oxidation of **46** (Table 1, entry 14) and in the significant (albeit modest) regioselectivity observed in oxidation of simple alkanes such as *n*-hexane and *n*-heptane (Table 1, entries 7 and 8).[65,66] Therefore, for these simple substrates the nature of the diamine backbone has a more decisive role than the cavity created by the relative orientation of the pinene rings in defining C−H regioselectivity on the basis of sterics. We conclude that the cyclohexyl *N*-methyl groups in **Λ-1P** and **Δ-1P** result in more effective steric constraints in close proximity to the iron site than those exerted by the bipyrrolidine (**Λ-2P** and **Δ-2P**).

In conclusion, the combination of observations points out **Λ-1P** and **Δ-1P** as very unique catalysts that sensitively respond to steric properties of C−H groups in these simple hydrocarbons, while providing good yields of alkyl C−H oxidized products.

Selective Oxidation of Complex Molecules. The potential utility of this family of catalysts in organic synthesis is best illustrated in the oxidation of structurally more complex substrates. The structurally rich nature of the complexes was envisioned to most sensitively affect yields and/or selectivities in the oxidation of these non-trivial molecules.

The selective oxidation of (−)-ambroxide (**50**) can be regarded as a non-trivial problem. This terpenoid contains 14 methylene and 2 tertiary C−H bonds (Figure 3a). It has been

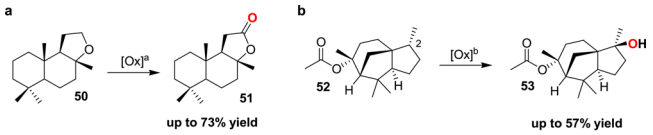

c

	Catalyst						
	Λ-1P	Δ-1P	Λ-2P	Δ-2P	Λ-2	Δ-2	$2SbF_6$
Substrate	Product yield %[c]						
50	73 (70)[d]	73	60	72	58	66	57[e]
52	56 (49)[d]	32	57	21	20	17	15[f]

[a] Cat:H_2O_2:substrate:AcOH; 3:260:100:150, rt. [b] 3:250:100:150, 0 °C. [c] GC yield based on substrate. [d] Isolated by flash chromatography. [e] **Δ-2SbF$_6$**. [f] **Λ-2SbF$_6$**.

Figure 3. Oxidation of complex molecules: (a) oxidation of (−)-ambroxide; (b) oxidation of (+)-cedryl acetate; (c) results of reactions a and b.

recently described that (−)-ambroxide (**50**) can be selectively oxidized at the activated methylene site adjacent to the ether moiety to yield (+)-sclareolide (**51**) in 80% yield by employing 15 mol % of **Λ-2SbF$_6$**.[52] However, when it is submitted to oxidation under analogous experimental low catalyst loading conditions (3 mol %) by the family of complexes **Λ-1P**, **Δ-1P**, **Λ-2P**, and **Δ-2P**, selective formation of (+)-sclareolide (**51**) is obtained in yields ranging from 60 to 73% (Figure 3c). Interestingly, the best product yields are obtained with pinene-containing catalysts **Λ-1P**, **Δ-1P**, and **Δ-2P**, but a clear relationship between catalyst structure and catalytic activity could not be identified, suggesting that optimum product yield results from a combination of factors.

The rigid bridged tricyclic sesquiterpene (+)-cedryl acetate (**52**) does not contain a powerful electronic directing group. From the three tertiary C−H bonds present, one is in a bridgehead and a second one is situated in a ring junction. Therefore, C2−H (Figure 3b) appears to be the least sterically hindered tertiary C−H site, and it is the most distant from the deactivating acetate group. When **52** was submitted to our standard experimental conditions, catalysts containing the well-defined cavity around the metal center (**Λ-1P** and **Λ-2P**) were the most efficient, furnishing hydroxylated product **53** in 56−57% yields. Modest yields are obtained with **Λ-2** and **Δ-2**

dx.doi.org/10.1021/jo302196q | J. Org. Chem. 2013, 78, 1421−1433

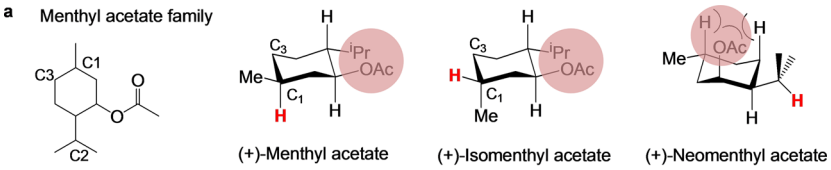

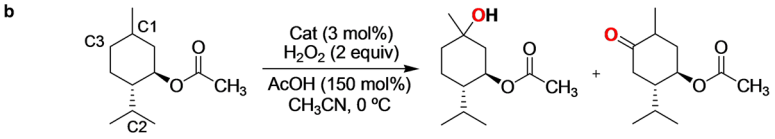

	Menthol and isomenthol derivatives		
	54	**3**	**60**
Catalyst	**Yield %[a] [M-OH1 / M-K][b]**		
Λ-1P	37 [86/13]	63 (65)[c] [95/5]	75 [86/14]
Δ-1P	58 [90/10]	42 [76/24]	83 [89/11]
Λ-2P	47 [85/15]	59 [88/12]	70 (63)[c] [83/17]
Δ-2P	52 [85/15]	47 [79/21]	65 [85/15]
Λ-2SbF$_6$	42 [78/22]	47 [83/17]	
Λ-2	45 [77/23][d]	48 [83/17][d]	
Δ-2	48 [84/16][d]	47 [78/22][d]	

[a] Combined GC yield based on substrate. [b] Normalized (100) ratio of products. [c] Isolated by flash chromatography. [d] Arrows connecting reactions of **Λ-2** and **Δ-2** with substrates **54** and **3** correspond to enantiomerically related reactions.

Figure 4. Oxidation of menthyl acetate family: (a) chair representations of (+)-menthyl acetate (**54**), (+)-isomenthyl acetate (**60**), and (+)-neomenthyl acetate (**69**).[68,69] The tertiary C−H groups preferentially oxidized are indicated in red. The pink shading indicates interactions that disfavor oxidation of the tertiary C−H groups involved. (b) Table of results.

(Figure 3c), and for comparison, it should be noted that oxidation with Gif reagents provides the product in 1% yield.[67]

Chiral Matching in C−H Oxidation Reactions. A set of derivatives of menthol was further identified as a test platform for studying selectivity in C−H oxidation responding to a combination of electronic, steric and chiral properties of the substrate, and the catalysts. Figure 4a shows the most stable conformational isomers for (+)-menthyl acetate (**54**), (+)-isomenthyl acetate (**60**), and (+)-neomenthyl acetate (**69**).[68,69] The conformational isomers shown in the figure are also assumed to be the most reactive (Curtin−Hammet principle) and to dominate the regioselectivity outcome of their oxidation.

For menthyl and isomenthyl esters, tertiary C−H bonds at C1 and C2 and the CH_2 in position C3 were identified as the electronically least deactivated positions. From the 3D chair structure (Figure 4a) it can be observed that the ester moiety is spatially close to the isopropyl group, and some steric hindrance of C2−H could be predicted. Menthyl and isomenthyl acetate differ uniquely in the disposition of the C1−H bond. In the first one, the C1−H bond is in axial disposition, while it is equatorial in the second. For this reason, we envisioned that the oxidation of the C1 position would be more efficient for isomenthyl acetate than for menthyl acetate. As expected, irrespective of the iron catalyst employed, menthyl and isomenthyl esters are oxidized preferentially in C1−H to the corresponding tertiary alcohol (Figure 4b). In addition, the ketone product resulting from oxidation at C3 is a minor product, and oxidation at C2 is observed in only trace amounts. Also as expected, the best yields and excellent selectivity toward C1−H were obtained in the oxidation of isomenthyl esters (Figure 4b and Table S11 (Supporting Information)). For example, the oxidation of (+)-isomenthyl acetate (**60**) proceeds to the corresponding tertiary alcohol with better yields (up to 83% for **Δ-1P**) than the oxidation of (+)-menthyl acetate (**54**) (up to 58% for **Δ-1P**; Figure 4b).

Comparative oxidation of optically pure + and − enantiomers of menthyl acetate allowed us to investigate if a stereoselective match between chiral catalyst and substrate could give rise to distinct selectivities and/or improved yields.

Effectively, as a general rule, complexes presenting a Λ chiral conformation such as **Λ-1P**, **Λ-2P**, and **Λ-2** showed better yields and selectivity for the tertiary alcohol at C1 (**M-OH1**) when reacting with **3** (− isomer). Instead, **54** (+ isomer) is more conveniently oxidized with complexes possessing Δ chirality (Figure 4b). The most remarkable differences are observed in the case of catalysts **Δ-1P** and **Λ-1P**. The latter is very selective and efficient in the oxidation of **3** (yield (%) [**M-OH1**/**M-K**] 65 [95/5]) but quite mediocre when reacting with **54** (yield (%) [**M-OH1**/**M-K**] 37 [86/13]). The opposite occurs with **Δ-1P** (yield (%) [**M-OH1**/**M-K**] 42 [76/24] and 58 [90/10], respectively). Moreover, in the oxidation of (+)-isomenthol acetate (**60**) **Δ-1P** provides better yield (83%) than **Λ-1P** (75%, Figure 4b).

dx.doi.org/10.1021/jo302196q | J. Org. Chem. 2013, 78, 1421−1433

In conclusion, for each substrate a leading catalyst can be identified in terms of yields and selectivity. However, irrespective of the catalyst, the dominant regioselectivity in these substrates is dictated by the relative inherent reactivities of the different C−H bonds.

Diverting Selectivity in C−H Oxidations. A more interesting case will be the oxidation of molecules where different activating or deactivating factors are in competition, and there is not only a single strongly favored C−H oxidation site. In these cases, it was envisioned that the toolset of iron catalysts could allow determination of the preferential C−H oxidation site.

Analysis of the chair-3D structure of neomenthol derivatives (**66**, **69**, **72** and **75** (Figure 5; see Figure 4a for chair-3D structure)) shows that in this case the ester group is in an axial

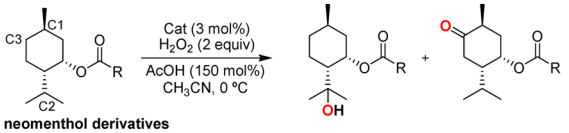

neomenthol derivatives

(-) and R=CH_3, **66**
(+) and R=CH_3, **69**
(+) and R=CF_3, **72**
(+) and R=tBu, **75**

N-OH2: **67**, **70**, **73**, **76**

N-K: **68**, **71**, **74**, **77**

	Neomenthol derivatives			
	66	**69**	**72**	**75**
Catalyst	**Yield %[a] (substrate conversion) [N-OH2 / N-K][b]**			
Λ-1P	40, 42[c] (53) [55/45]	43 (77) [83/17]	35, 35[c] (64) [83/17]	54 (71) [80/20]
Δ-1P	44 (59) [64/36]	41 (51) [44/56]	34 (40) [61/39]	40 (44) [34/66]
Λ-2P	47 (72) [58/42]	43 (74) [69/31]	41 (96) [53/47]	46, 45[c] (66) [52/48]
Δ-2P	43 (69) [48/52]	44 (68) [44/56]	34 (72) [42/58]	35 (48) [34/66]
Λ-2SbF$_6$	43 (70) [41/59]	46 (66) [48/52]		
Λ-2	43 (69) [42/58]	44 (66) [49/51]	33 (61) [40/60]	38 (50) [40/60]
Δ-2	44 (72) [48/52]	44 (72) [42/58]	33 (64) [37/63]	34 (43) [35/65]

[a] Combined GC yield based on substrate [b] Normalized (100) ratio of products. [c] Isolated by flash chromatography.

Figure 5. Oxidation of neomenthol derivatives.

position and provides steric hindrance for the axial C−H bond at C1. In addition, because of the axial orientation of the acetate group, the tertiary C−H site at C2 is not effectively shielded and becomes spatially more accessible. This analysis predicts that two distinct sites are most prone for oxidation; these are the tertiary C−H group at C2 to form alcohol **N-OH2**, and methylene C−H at C3 to yield ketone **N-K**, which are the most distant from the electron-withdrawing acetate group. Since neither of these two positions appear to be strongly favored, these substrates are a convenient platform for exploring regioselectivity tuning responding to catalyst structure.

As predicted, oxidation of these substrates with the full family of catalysts (Figure 5) yields two major oxidation products: the tertiary alcohol resulting from oxidation at C2−H and the ketone resulting from oxidation at C3. Interestingly, the regioselectivity also depends on the relative chirality of the substrate and the catalyst. The simplest case to analyze is the oxidation of (−)-neomenthyl acetate (**66**) and (+)-neomenthyl acetate (**69**) by **Λ-2**, **Λ-2SbF$_6$**, and **Δ-2** catalysts. In all cases, similar amounts of **N-OH2** and **N-K** are obtained (Figure 5), the ketone being slightly favored. This small selectivity toward **N-K** is slightly higher when (−)-neomenthyl acetate (**66**) is oxidized with **Λ-2** or (+)-neomenthyl acetate (**69**) is oxidized with **Δ-2**. In addition, **Λ-2** and **Λ-2SbF$_6$** exhibit analogous yields and selectivities, suggesting that the anion in these two complexes has no influence on their relative activity.

Use of the more structurally elaborated pinene-containing catalysts allows modulating selectivity in a remarkable manner (Figure 5). Most significantly, pinene-containing complexes with Λ chirality divert C−H regioselectivity in the oxidation of (+)-neomenthyl acetate (**69**) toward the tertiary C2−H bond and reach an excellent selectivity with **Λ-1P** (yield (%) [**N-OH2**/**N-K**] 43 [83/17]). Interestingly, the high regioselectivity depends on the chirality of the substrate, and oxidation of (−)-neomenthyl acetate (**66**) with **Λ-1P** and **Λ-2P** proceeds with substantially smaller selectivity.

In general, when the acetate group is replaced by bulkier groups such as trifluoroacetate and pivalate (**72** and **75**, respectively), a significant increase in the relative C−H selectivity toward the ketone product is observed. In both cases, this effect probably responds to a greater steric hindrance of these groups, which are situated in spatial proximity to the isopropyl moiety. On the other hand, the electron-withdrawing nature of the trifluoroacetate group may exert some deactivation in the closer C2−H site.

Therefore, the oxidation of neomenthyl esters with the family of complexes **Λ-1P**/**Δ-1P**, **Λ-2P**/**Δ-2P** serves to illustrate the apparent ability of these highly structured catalysts to divert regioselectivity between a tertiary and a secondary C−H site in natural product derivatives. Nevertheless, a cautious note has to be made, as some of the reactions exhibit deficient mass balance and therefore overoxidation reactions may have influenced the final regioselectivities attained.

In order to further illustrate the potential synthetic utility of this selectivity, selected oxidation reactions of (+)-neomenthol derivatives were scaled up to millimole scale, with experimental conditions chosen to favor oxidation at C2−H and C3−H (Figure 6a). (+)-Neomenthyl pivalate **75** (0.7 mmol) was oxidized using **Λ-1P** (2 × 3 mol %), yielding tertiary alcohol **76** in 48% yield (along with 10% yield of ketone **77**). Alternatively, by using **Δ-1P** (3 × 3 mol %), ketone **77** was obtained as the main oxidation product in 29% yield (along with 20% yield of alcohol **76**). The regioselectivity obtained in these larger scale reactions (Figure 6a) is in reasonable agreement with that observed when smaller scale reactions are performed (Figure 5).

An even more challenging possibility would be to apply these iron catalysts to direct oxidation among multiple nonactivated methylene sites in complex organic molecules. Toward this end, (+)-sclareolide (**51**) was chosen as a test. In this case, the carbonyl group deactivates the surrounding C−H bonds, directing the oxidation toward the most remote cyclohexane ring, which contains three chemically distinct methylene sites (Figure 7). Preferential functionalization at C2 was described with catalyst **Δ-2SbF$_6$**[52] and in rhodium-catalyzed nitrene insertions.[64] Mn-porphyrin-mediated halogenations of (+)-sclareolide can be preferentially directed toward C2 and C3, depending on the porphyrin catalyst.[71] In all of these reactions, C−H selectivity among C1, C2, and C3 positions has been understood to be governed by steric factors.

When (+)-sclareolide is subjected to oxidation using **Λ-1P**, **Δ-1P**, **Λ-2P**, **Δ-2P**, **Λ-2**, and **Δ-2** as catalysts, ketone products (**78**−**80**, Figure 7) arising from oxidation at three different methylene sites (C1, C2, and C3, respectively) are obtained. A particularly excellent yield (up to 78%) is furnished with catalyst **Λ-1P**. Most surprisingly, site selectivity in the oxidation of (+)-sclareolide appears to be dependent on the nature of the catalyst, and the set of pinene-containing complexes (**Λ-1P**, **Δ-1P**, **Λ-2P**, **Δ-2P**) allow discrimination and diversion of the

dx.doi.org/10.1021/jo302196q | J. Org. Chem. 2013, 78, 1421−1433

a

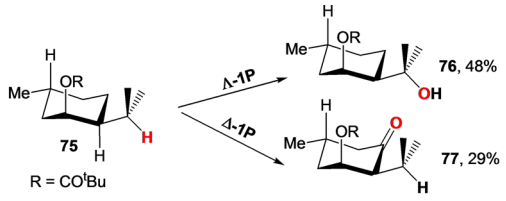

Yield %[a]					
Catalyst	76	77	Total	76/77	Conversion
Λ-1P[b]	48	10	58	83/17	91%
Δ-1P[c]	20	29	49	41/59	89%

[a] 0 °C. Cat:H_2O_2:substrate:AcOH; [b] (3)x2:(200)x2:100:(150)x2. [c] (3)x3:(200)x3:100:(150)x3.

b

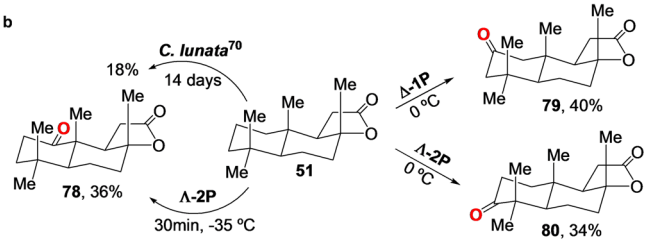

Yield %					
Catalyst (T)	78	79	80	Total	Conversion
Λ-2P (-35 °C)[a]	36	4	19	59	77%
Δ-1P (0 °C)[a]	7	40	26	73	89%
Λ-2P (0 °C)[b]	23	16	34	73	87%

Cat:H_2O_2:substrate:AcOH; [a] (3)x2:(340)x2:100:(150)x2. [b] 3:340:100:150.

Figure 6. Diverting selectivity in the oxidation: (a) **75** as substrate; (b) **51** as substrate.[70]

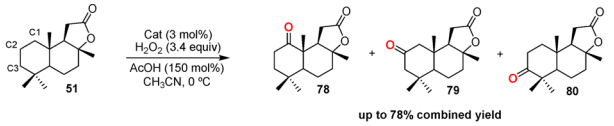

Catalyst						
Λ-1P	Δ-1P	Λ-2P	Δ-2P	Λ-2	Δ-2	Δ-2SbF_6
Product yield %[a] [78/79[b]/80][c]						
65 [36/37/27]	61 [7/63/30]	73 (78)[d] [28/25/47]	52 [17/42/41]	51 [11/45/44]	51 [18/43/39]	51 [16/43/41]

[a] Combined GC yield based on substrate. [b] C2-alcohol is also included. [c] Normalized (100) ratio of products. [d] Isolated by flash chromatography.

Figure 7. Oxidation of (+)-sclareolide.

dominant regioselectivity among multiple methylene sites. Such a change in site selectivity cannot be attained with the structurally simpler catalysts **Λ-2** and **Δ-2** (Figure 7); under our conditions, **Λ-2** and **Δ-2** afford the ketones (+)-2-oxosclareolide (**79**) and (+)-3-oxosclareolide (**80**), arising from preferential oxidation at C2 and C3 in roughly 1:1 relative ratios, accounting for more than 80% of the oxidized products obtained. Interestingly, in the case of catalyst **Λ-2P**, the regioselectivity can be further modulated by lowering the temperature, and at −35 °C ketone (+)-1-oxosclareolide (**78**) becomes the dominant product. This observation suggests that reactions are not under thermodynamic control. Unfortunately, the rest of the catalysts are basically inactive (<5% conversion) at this low temperature.

To probe the synthetic value of these observations, oxidation of (+)-sclareolide was scaled up to millimole scale using experimental conditions that favor ketones **78**−**80** (Figure 6b). These can be obtained as the main products in yields of 36% (61% selectivity), 40% (55% selectivity), and 34% (47% selectivity), respectively, by choosing the appropriate experimental conditions and catalyst.

We conclude that this family of catalysts allows the late-stage oxidation of a complex organic molecule toward three different ketone products by means of selective methylene oxidation. While overall yields could be regarded as modest, they are still suitable for preparative purposes and their value becomes most evident when considering that functionalization of C1 has not been described for any synthetic catalyst. Indeed, (+)-1-oxosclareolide (**78**) is only available in low yields via biotransformations by filamentous fungi (*A. niger*, *C. blackesleeana*, and *C. lunata*; 10%, 9%, and 18% yields, respectively),[70] at much longer reaction times (14 days) than for our system. In addition, to the best of our knowledge, the switch in selectivity among distinct methylene sites using nonenzymatic reagents finds exclusive precedent in shape-selective oxidations with sterically hindered metalloporphyrins.[65,72]

CONCLUSION

Pinene-containing non-heme iron catalysts **Λ-1P**, **Δ-1P**, **Λ-2P**, and **Δ-2P** mediate the fast oxidation of nonactivated tertiary and secondary alkyl moieties under mild experimental conditions in synthetically amenable yields, employing H_2O_2 as oxidant, without requiring an excess of the substrate. Steric hindrance at the iron active site confers stability toward catalyst degradation pathways. This stability enables the use of low catalyst loadings. Complex organic molecules are oxidized in good yields and selectivity. Simple rules previously established for alkyl C−H functionalization with electrophilic reagents can be used to predict which C−H groups may be more prone to oxidation. Unlike most synthetic C−H oxidation reagents, the present catalysts are highly structured. Interestingly, this key feature allows for modulating or even altering selectivity without the use of covalent or strong supramolecular substrate−oxidant interactions. Therefore, the final selectivity outcome depends on a combination of more subtle aspects mainly affecting the spatial structure of the iron active site. The chirality of the catalysts, the nature of the ligand diamine backbone, and the presence of a cavity-like site surrounding the iron center have been identified as structural aspects that translate into C−H site selectivity.

A cautious note must be made at this point. It is quite illustrative to remark that changes in regioselectivity dictated by the nature and chirality of the diamine or the orientation of the pinene correspond to very modest variations in the relative energies of the paths leading to oxidation of the different C−H groups. Therefore, interpretation and predictability needs caution. Nevertheless, changes in selectivity ratios between the oxidation of tertiary and secondary C−H groups and also among multiple methylene sites are shown to be useful for providing oxidation products in synthetically valuable yields. Furthermore, regioselectivities obtained with these Fe-based catalysts are important because they are complementary to those that can be reached with other oxidizing reagents,[16−21,73,74] thus expanding the possibilities of C−H functionalization as a tool for simplifying chemical synthesis.

EXPERIMENTAL SECTION

Synthesis of Complexes. *Δ-[$FeCl_2$((R,R,R)-MCPP)].* Under a N_2 atmosphere, $FeCl_2$ (25 mg, 0.198 mmol) was added to a stirred solution of (*R,R,R*)-MCPP (100.0 mg, 0.198 mmol) in THF (5 mL).

dx.doi.org/10.1021/jo302196q | J. Org. Chem. 2013, 78, 1421−1433

The reaction mixture was stirred overnight to obtain an orange jelly. The solvent was evaporated under reduced pressure, and the resulting solid was redissolved with CH_2Cl_2 and the solution filtered. Slow diffusion of diethyl ether into the solution led to the formation of 40 mg (0.062 mmol, 63%) of orange crystals after 2 days. Anal. Calcd for $C_{34}H_{48}Cl_2FeN_4{\cdot}0.6CH_2Cl_2$ (MW = 639.53 g/mol): N, 8.11; C, 60.19; H, 7.18. Found: N, 8.39; C, 59.99; H, 7.06. FT-IR (ATR; ν, cm^{-1}): 2969−2867 $(C-H)_{sp^3}$, 1736, 1616, 1560, 1489, 1473, 1454, 1422, 1356, 1270, 1253, 1107, 1020, 975, 956, 925, 873, 724. ^1H NMR (400 MHz, CD_3CN, 300 K; δ, ppm): 138 (s), 107 (s), 48.4 (s), 47.5 (s), 16.8 (s), 9.98−0.89 (m), −6.0 (s), −23.5 (s). ESI-MS (m/z): 603.3 (100) $[M - Cl]^+$, 284.1 (25) $[M - 2Cl]^{2+}$. UV (CH_3CN; λ_{max}, nm (ε, M^{-1} cm^{-1})): 270 (5518), 330 (sh), 419 (1114). CV: $E_{1/2}$ (ΔE) 101 mV (106). X-ray analysis indicates that the complex adopts a Δ topological chirality.

*Δ-[Fe(CF_3SO_3)$_2$((R,R,R)-MCPP)] (**Δ-1P**).* Under a N_2 atmosphere, to a stirred mixture of Δ-[$FeCl_2$((*R*,*R*,*R*)-MCPP)] (50.0 mg, 0.08 mmol) in CH_2Cl_2 (1.5 mL) was added a suspension of $AgCF_3SO_3$ (40.7 mg, 0.16 mmol) in CH_2Cl_2 (1.5 mL). The mixture was stirred for 3 h and then filtered through Celite to remove the precipitated AgCl. The solvent was removed under reduced pressure and the resulting solid dissolved in 1 mL of CH_2Cl_2. Slow diffusion of diethyl ether into the solution led to the formation of 41 mg (0.048 mmol, 60%) of yellow crystals after 2 days. Anal. Calcd for $C_{36}H_{48}F_6FeN_4O_6S_2{\cdot}0.15CH_2Cl_2$ (MW = 879.44 g/mol): N, 6.37; C, 49.37; H, 5.54; N, 7.29. Found: N, 6.71; C, 49.08; H, 5.61; S, 7.04. FT-IR (ATR; ν, cm^{-1}): 2935−2875 $(C-H)_{sp3}$, 1289 (Py), 1236, 1217, 1160, 1026, 634 (CF_3SO_3). ^1H NMR (400 MHz, CD_2Cl_2, 300 K; δ, ppm): 167 (s), 112 (s), 66.5 (s), 50 (s), 25 (s), 19 (s), 9.7−0.1(m). ESI-MS (m/z): 717.2 (100) $[M - CF_3SO_3]^+$, 284.9 (20) $[M - 2CF_3SO_3]^{+2}$. UV (CH_3CN; λ_{max}, nm (ε, M^{-1} cm^{-1})): 256 (sh), 265 (sh), 377 (5448).

*Λ-[Fe(CF_3SO_3)$_2$((S,S,R)-BPBPP)] (**Λ-2P**).* A suspension of Fe(CH_3CN)$_2$(CF_3SO_3)$_2$ (130 mg, 0.30 mmol) in THF (2 mL) was added dropwise to a vigorously stirred solution of (*S*,*S*,*R*)-BPBPP (138 mg, 0.30 mmol) in THF (1 mL). The pale yellow precipitate that formed after stirring overnight was filtered. Diethyl ether was added to the resulting solution to ensure the complete precipitation of the product. This solid was added to that previously filtered and dissolved in CH_2Cl_2 (2 mL), and the solution was filtered again. Slow diethyl ether diffusion over the solution afforded, after a couple of days, the product as pale yellow crystals suitable for X-ray diffraction (152 mg, 0.176 mmol, 59%). Anal. Calcd for $C_{36}H_{46}F_6FeN_4O_6S_2{\cdot}0.1Et_2O$ (MW = 872.15 g/mol): N, 6.42; C, 50.13; H, 5.43; S, 7.35. Found: N, 6.72; C, 50.36; H, 5.25; N, 7.55. FT-IR (ATR; ν, cm^{-1}): 2990−2908 $(C-H)_{sp^3}$, 1315 (Py), 1236, 1215, 1157, 1027, 632 (CF_3SO_3). ^1H NMR (400 MHz, CD_2Cl_2, 300 K; δ, ppm): 182 (S), 117 (s), 76 (s), 51 (s), 32.3 (s), 28.8 (s), 21.8−17.4 (m), 7.9 to −6 (m), −8.3 (s), −20.6 (s). ESI-MS (m/z): 715.3 (100) $[M - CF_3SO_3]^+$, 283.1 (50) $[M - 2CF_3SO_3]^{+2}$. UV (CH_3CN; λ_{max}, nm (ε, M^{-1} cm^{-1})): 256 (sh), 265 (sh), 376 (6301). X-ray analysis indicates that the complex adopts a Λ topological chirality.

*Δ-[Fe(CF_3SO_3)$_2$((R,R,R)-BPBPP] (**Δ-2P**).* The same procedure as for complex **Λ-2P** gave **Δ-2P** as yellow crystals (147 mg, 0.170 mmol, 57%). Anal. Calcd for $C_{36}H_{46}F_6FeN_4O_6S_2{\cdot}H_2O$ (MW = 882.75 g/mol): N, 6.35; C, 48.99; H, 5.48; S, 7.25. Found: N, 6.39; C, 48.88; H, 5.40; S, 7.10. FT-IR (ATR; ν, cm^{-1}): 2987−2873 $(C-H)_{sp3}$, 1312 (Py), 1235, 1216, 1158, 1029, 630 (CF_3SO_3). ^1H NMR (400 MHz, CD_2Cl_2, 300 K; δ, ppm): 176 (S), 118 (s), 79 (s), 49 (s), 33.7 (s), 28.3 (s), 18.3 (sa), 8.2 to −2 (m), −8.1 (s), −15.9 (s). ESI-MS (m/z): 715.3 (100) $[M - CF_3SO_3]^+$, 283.1 (80) $[M - 2CF_3SO_3]^{+2}$. UV (CH_3CN; λ_{max}, nm (ε, M^{-1} cm^{-1})): 257 (sh), 265 (sh), 378 (5550). X-ray analysis indicates that the complex adopts a Δ topological chirality.

Synthesis of Substrates. Synthesis of **9**, **13**, and **22**[51] was carried out as previously described.

*(−)-Menthyl Trifluoroacetate (**57**).* (−)-Menthol (2.50 g, 16.0 mmol), 1-methylimidazole (1.5 mL), and trifluoroacetic anhydride (15 mL) were dissolved in CH_3CN (30 mL) and stirred for 24 h at room temperature. Ice (25 mL) was added at this point. After the mixture was stirred for 15 min, $CHCl_3$ (60 mL) was added. The organic layer was washed with 1 M H_2SO_4 (25 mL) and a mixture of water (23 mL) and saturated $NaHCO_3$ solution (2 mL) (four times, until neutral pH) and dried over $MgSO_4$, and the solvent was removed under reduced pressure. Purification over silica (hexane/ethyl acetate 95/5) yielded 3.05 g of the product as a colorless oil (75% yield). FT-IR (ATR; ν, cm^{-1}): 2959, 2930, 2874, 1776, 1218, 1161, 1143, 947, 729. ^1H NMR (400 MHz, $CDCl_3$, 300 K; δ, ppm): 4.87 (td, J = 11.0, 4.5 Hz; 1H), 2.07−2.04 (m, 1H), 1.89−1.81 (m, 1H), 1.76−1.72 (m, 2H), 1.56−1.50 (m, 2H), 1.18−1.12 (m, 2H), 0.97−0.88 (m, 1H), 0.94 (d, J = 6.6 Hz, 3H), 0.92 (d, J = 7.0 Hz, 3H), 0.78 (d, J = 7.0 Hz, 3H). ^{13}C NMR (100 MHz, $CDCl_3$, 300 K; δ, ppm): 157.2, 114.7, 79.3, 46.7, 40.0, 33.9, 31.4, 26.2, 23.4, 21.8, 20.5, 16.1. HRMS (ESI-TOF, $[M + Na]^+$): m/z calcd for $C_{12}H_{19}F_3O_2Na$ 275.1223, found 275.1216.

*(+)-Isomenthyl Acetate (**60**).* (+)-Isomenthol (5.0 g, 30.7 mmol), 1-methylimidazole (3.5 mL), and acetic anhydride (35 mL) were dissolved in CH_3CN (60 mL) and stirred for 30 min at room temperature. Ice (50 mL) was added at this point. After the mixture was stirred for 15 min, $CHCl_3$ (125 mL) was added. The organic layer was washed with 1 M H_2SO_4 (50 mL), saturated $NaHCO_3$ solution (50 mL), and water (50 mL) and dried over $MgSO_4$, and the solvent was removed under reduced pressure. Purification by flash chromatography over silica (hexane/ethyl acetate 2/1) yielded 4.79 g of the product as a colorless oil (79% yield). FT-IR (ATR; ν, cm^{-1}): 2956, 2929, 2871, 1730, 1368, 1239, 1028. ^1H NMR (400 MHz, $CDCl_3$, 300 K; δ, ppm): 5.03 (td, J = 6.8, 3.7 Hz, 1H), 2.03 (s, 3H), 1.89−1.86 (m, 1H), 1.76−1.71 (m, 1H), 1.60−1.54 (m, 2H), 1.52−1.43 (m, 3H), 1.32−1.22 (m, 2H), 0.93 (d, J = 6.8 Hz, 3H), 0.92 (d, J = 6.9 Hz, 3H), 0.85 (d, J = 6.6 Hz, 3H). ^{13}C NMR (100 MHz, $CDCl_3$, 300 K; δ, ppm): 170.6, 71.5, 45.8, 35.9, 30.0, 27.5, 26.3, 21.4, 20.9, 20.7, 20.4, 18.9. HRMS (ESI-TOF, $[M + Na]^+$): m/z calc for $C_{12}H_{22}O_2Na$ 221.1512, found 221.1515.

*(+)-Isomenthyl Pivalate (**63**).* (+)-Isomenthol (5.0 g, 30.7 mmol) and 4-(dimethylamino)pyridine (360 mg) were dissolved in pyridine (50 mL). The resulting mixture was cooled in an ice bath, and a solution of pivaloyl chloride (4.2 mL, 33.5 mmol) in pyridine (30 mL) was added dropwise. After the mixture was stirred for 24 h, the solvent was removed under reduced pressure and the resulting residue was treated with $CHCl_3$ (250 mL) and washed with water (100 mL), saturated $NaHCO_3$ aqueous solution (100 mL), and saturated NaCl aqueous solution (100 mL). The organic phase was dried over $MgSO_4$ and filtered, and the solvent was removed under reduced pressure to yield a colorless liquid. Purification by flash chromatography over silica (hexane/ethyl acetate 7/1) followed by flash chromatography over alumina (hexane) yielded 4.81 g of the product as a colorless oil (65% yield). FT-IR (ATR; ν, cm^{-1}): 2957, 2930, 2872, 1723, 1283, 1163, 1138. ^1H NMR (400 MHz, $CDCl_3$, 300 K; δ, ppm): 5.01 (dt, J = 6.2, 3.4, 1H), 1.88−1.82 (m, 1H), 1.78−1.70 (m, 1H), 1.60−1.41 (m, 6H), 1.35−1.26 (m, 1H), 1.19 (s, 9H), 0.94 (d, J = 6.6 Hz, 3H), 0.91 (d, J = 7.1 Hz, 3H), 0.85 (d, J = 6.7 Hz, 3H). ^{13}C NMR (100 MHz, $CDCl_3$, 300 K; δ, ppm): 177.9, 71.3, 45.4, 38.8, 35.5, 29.9, 27.5, 27.1, 26.2, 21.0, 20.9, 20.8, 19.3. HRMS (ESI-TOF, $[M + Na]^+$): m/z calcd for $C_{15}H_{28}O_2Na$ 263.1981, found 263.1969.

*(+)-Neomenthyl Fluoroacetate (**72**).* The same procedure was used as for **57**. Purification over silica (hexane/ethyl acetate 95/5). 2.97 g of colorless oil obtained (73% yield). FT-IR (ATR; ν, cm^{-1}): 2955, 2929, 1778, 1331, 1217, 1160, 1137. ^1H NMR (400 MHz, $CDCl_3$, 300 K; δ, ppm): 5.41−5.40 (m, 1H), 2.05−2.00 (m, 1H), 1.81−1.77 (m, 2H), 1.65−1.59 (m, 1H), 1.48−1.33 (m, 2H), 1.2−1.04 (m, 2H), 1.12−0.95 (m, 1H), 0.92 (d, J = 6.7 Hz, 3H), 0.89 (d, J = 6.6 Hz, 3H), 0.88 (d, J = 6.7 Hz, 3H). ^{13}C NMR (100 MHz, $CDCl_3$, 300 K; δ, ppm): 157.0, 114.7, 76.9, 46.6, 38.6, 34.4, 29.0, 26.3, 24.7, 21.9, 20.7, 20.5. HRMS (ESI-TOF, $[M + Na]^+$): m/z calcd for $C_{12}H_{19}F_3O_2Na$ 275.1223, found 275.1199.

*(+)-Neomenthyl Pivalate (**75**).* The same procedure was used as for **63**. Purification by flash chromatography over silica (hexane). 5.55 g of colorless oil obtained (75% yield). FT-IR (ATR; ν, cm^{-1}): 2954, 2920, 2870, 1723, 1478, 1284, 1164, 1142.^1H NMR (400 MHz, $CDCl_3$, 300 K; δ, ppm): 5.15−5.12 (m, 1H), 1.96−1.89 (m, 1H), 1.80−1.72 (m, 2H) 1.65−1.52 (m, 1H), 1.47−1.25 (m, 2H), 1.20 (s, 9H), 1.65−0.91 (m, 3H), 0.89 (d, J = 6.7 Hz, 3H), 0.85 (d, J = 6.5 Hz, 3H), 0.84 (d,

dx.doi.org/10.1021/jo302196q | J. Org. Chem. 2013, 78, 1421−1433

J = 6.6 Hz, 3H). ^{13}C NMR (100 MHz, $CDCl_3$, 300 K; δ, ppm): 177.8, 70.5, 47.0, 39.1, 39.0, 34.8, 29.3, 27.2, 26.6, 25.4, 22.2, 21.1, 20.6. HRMS (ESI-TOF, $[M + Na]^+$): m/z calcd for $C_{15}H_{28}O_2Na$ 263.1981, found 263.1967.

Reaction Conditions for Catalysis. All liquid substrates were purified by passing through an alumina plug immediately before being used.

Sample Analysis. GC analysis of the catalysis provided substrate conversions and product yields relative to the internal standard integration. Calibration curves were obtained from commercial products when available, or from pure isolated products obtained from previously reported procedures (**10**, **14**, **15**, **20**, **21**, **23**, **24**, **39**, **55**;[51] **33**, **34**[52]) or from catalytic reactions described below.

*Time-Profile Experiments. Procedure for Obtaining the Profiles of the Catalytic Oxidation of (1R)-(−)-Menthyl Acetate (**3**) and cis-1,2-Dimethylcyclohexane (**6**): Two-Step Addition of H_2O_2 To Prove the Relative Stability of the Catalysts in the Presence of a Large Excess of Substrate.* A 5 mL vial was charged with catalyst (7 μmol, 1 mol %), substrate (700 μmol, 1 equiv), CH_3CN (4.7 mL), and a magnetic stir bar. The vial was placed in an ice bath, and the contents were stirred. A 1.74 M CH_3CO_2H solution in CH_3CN was added (197 μL, 350 μmol, 50 mol %), and 560 μL of a 1.5 M (840 μmol, 1.2 equiv) H_2O_2 solution (diluted from a 35% H_2O_2 aqueous solution) was delivered by syringe pump over 6 min at 0 °C. After syringe pump addition, the resulting solution was stirred for another 6 min. At this point 4 equiv of substrate (2.8 mmol) was added and a second addition of H_2O_2 (560 μL of 1.5 M, 840 μmol, 1.2 equiv, starting time of second addition 12.5 min) was delivered by syringe pump over 6 min. After syringe pump addition, the resulting solution was stirred for another 6 min. Samples (100 μL) of the crude reaction were taken at different times and immediately passed through a short alumina plug along with the internal standard, followed by elution with 0.5 mL of AcOEt. Finally, the solution was subjected to GC analysis.

*Iterative Addition Protocol. Substrate: cis-4-Methylcyclohexyl-1-pivalate (**9**, Three Additions) and Cyclohexane (**11**, Two Additions).* A 5 mL vial was charged with catalyst (1 μmol, 1 mol %), the substrate (100 μmol, 1 equiv), CH_3CN (0.67 mL), and a magnetic stir bar. The vial was placed in an ice bath, and the contents were stirred. A 1.74 M CH_3CO_2H solution in CH_3CN was added (29 μL, 50 μmol, 50 mol %), and 80 μL of a 1.5 M (120 μmol, 1.2 equiv) H_2O_2 solution (diluted from a 35% H_2O_2 aqueous solution) was delivered by syringe pump over 6 min at 0 °C. After syringe pump addition, the solution was stirred for 10 min at 0 °C and a solution of catalyst (1 μmol, 1 mol %), CH_3CN (0.67 mL), and CH_3CO_2H (29 μL 1.74 M solution, 50 μmol, 50 mol %) was added simultaneously with 80 μL of a 1.5 M (120 μmol, 1.2 equiv) H_2O_2 solution via syringe pump over 6 min. After syringe pump addition the resulting solution was stirred for another 10 min.

If a third addition was required, a solution of catalyst (1 μmol, 1 mol %), CH_3CN (0.67 mL), and CH_3CO_2H (29 μL 1.74 M solution, 50 μmol, 50 mol %) was added simultaneously with 80 μL of a 1.5 M (120 μmol, 1.2 equiv) H_2O_2 solution via syringe pump over 6 min. After syringe pump addition the resulting solution was stirred for another 10 min.

An internal standard was added at this point. The iron complex was removed by passing the solution through a short path of silica followed by elution with 2 mL of AcOEt. Finally, the solution was subjected to GC analysis.

*Single-Addition Protocol. Substrate: cis-1,2-Dimethylcyclohexane (**6**) and 2,6-Dimethyloctane (**16**).* A 5 mL vial was charged with catalyst (1.2 μmol, 1 mol %), substrate (120 μmol, 1 equiv.), CH_3CN (0.8 mL), and a magnetic stir bar. A 1.74 M CH_3CO_2H solution in CH_3CN was added (35 μL, 60 μmol, 150 mol %), the vial was placed in an ice bath, and the contents were stirred. A 1.5 M (144 μmol, 1.2 equiv for **6**; 216 μmol, 1.8 equiv for **16**) H_2O_2 solution (diluted from a 35% H_2O_2 aqueous solution) was delivered by syringe pump over 6 min at 0 °C. After syringe pump addition, the resulting solution was stirred for another 10 min. Biphenyl was added at this point as internal standard. The iron complex was removed by passing the solution through a short path of silica followed by elution with 2 mL of AcOEt. Finally, the solution was subjected to GC analysis.

Substrate: Several. A 5 mL vial was charged with catalyst (1.2 μmol, 3 mol %), substrate (40 μmol, 1 equiv), CH_3CN (0.8 mL), and a magnetic stir bar. A 1.74 M CH_3CO_2H solution in CH_3CN was added (35 μL, 60 μmol, 150 mol %), the vial was placed in an ice bath, and the contents were stirred. The necessary amount of a 1.5 M (X equiv; see Table 2) H_2O_2 solution (diluted from a 35% H_2O_2 aqueous solution) was delivered by syringe pump over 17 min at 0 °C. After syringe pump addition, the resulting solution was stirred for another 10 min. Biphenyl was added at this point as internal standard. The iron complex was removed by passing the solution through a short path of silica followed by elution with 2 mL of AcOEt. Finally, the solution was subjected to GC analysis.

Table 2. Conditions for the Oxidation of Several Substrates

cat:H_2O_2:substrate:AcOH (equiv of H_2O_2)	substrate
3:200:100:150 (2)	**3, 9, 13, 16, 19, 22, 35, 38, 54, 57, 60, 63, 66, 69, 72, 75**
3:250:100:150 (2.5)	**52**
3:260:100:150 (2.6)	**50** (room temp)
3:280:100:150 (2.8)	**11, 42**
3:320:100:150 (3.2)	**25, 28, 32, 46**
3:340:100:150 (3.4)	**51** (different temp)

Procedure for Product Isolation. A 25 mL round-bottom flask was charged with catalyst (12 μmol, 3 mol %), alkane (0.4 mmol, 1 equiv), CH_3CN (8 mL), and a magnetic stir bar. A 1.74 M CH_3CO_2H solution in CH_3CN was added (0.35 mL, 0.6 mmol, 150 mol %), the mixture was placed in an ice bath, and the contents were stirred. The necessary amount of a 1.5 M (X equiv; see Table 2) H_2O_2 solution (diluted from a 35% H_2O_2 aqueous solution) was delivered by syringe pump over 17 min at 0 °C. After syringe pump addition, the solution was stirred for 10 min at 0 °C. Solvent was removed under reduced pressure, and the resulting residue was purified by flash chromatography on silica gel. The urity of the obtained products was checked by ^{1}H NMR and GC, and yields were corrected onthe basis of these results.

4: purification by flash chromatography over silica (hexane). Yield: 52.9 mg (62%) using **Λ-1P**. ^{1}H NMR (400 MHz, $CDCl_3$, 300 K; δ, ppm): 5.03−4.96 (m, 1H), 2.07−2.00 (m, 1H) 2.03 (s, 3H), 1.93−1.85 (m, 1H), 1.71−1.65 (m, 1H), 1.55−1.32 (m, 5H), 1.24 (s, 3H), 0.92 (d, J = 7.0 Hz, 3H), 0.80 (d, J = 7.1 Hz, 3H); in agreement with those reported in the literature.[52]

5: purification by flash chromatography over silica (hexane). Yield: 2.8 mg (3.2%) using **Λ-1P**. FT-IR (ATR; ν, cm^{-1}): 2958, 2928, 2872, 1714, 1365, 1235, 1030, 803. ^{1}H NMR (400 MHz, $CDCl_3$, 300 K; δ, ppm): 5.11−5.03 (m, 1H), 2.58−2.47 (m, 1H) 2.39−2.30 (m, 2H), 2.21−2.11 (m, 1H), 2.08 (s, 3H), 1.99−1.87 (m, 2H), 1.47−1.36 (m, 1H), 1.03 (d, J = 6.6 Hz, 3H), 0.89 (d, J = 6.7 Hz, 3H), 0.83 (d, J = 6.7 Hz, 3H). ^{13}C NMR (100 MHz, $CDCl_3$, 300 K; δ, ppm): 211.2, 170.6, 71.4, 47.8, 42.0, 39.2, 38.4, 26.6, 21.2, 20.3, 15.7, 14.1. HRMS (ESI-TOF, $[M + Na]^+$): m/z calcd for $C_{12}H_{20}O_3Na$ 235.1305, found 235.1297.

10: purification by flash chromatography over silica (hexane/AcOEt 3/1). Yield: 48.9 mg (57%) using **Λ-1P**. ^{1}H NMR (400 MHz, $CDCl_3$, 300 K; δ, ppm): 4.93 (m, 1H), 1.91−1.85 (m, 2H), 1.72−1.63 (m, 4H), 1.54−1.50 (m, 2H), 1.27 (s, 3H), 1.20 (s, 9H); in agreement with those reported in the literature.[51]

51: after reaction, 1 equiv of HCl (2 M) was added and the crude mixture heated to 40 °C for 4 h to reverse partial lactone ring opening. Purification by flash chromatography over silica (hexane) afforded 70.1 mg (70%) using **Λ-1P**. ^{1}H NMR (400 MHz, $CDCl_3$, 300 K; δ, ppm): 2.44−2.36 (m, 1H), 2.26−2.20 (m, 1H), 2.08−2.05 (m, 1H), 1.99−1.93 (m, 1H), 1.90−1.83 (m, 1H), 1.75−1.57 (m, 2H), 1.50−0.96 (m, 7H), 1.33 (s, 3H), 0.91 (s, 3H), 0.87 (s, 1H), 0.83 (s, 3H); in agreement with those of the commercially available product.

dx.doi.org/10.1021/jo302196q | J. Org. Chem. 2013, 78, 1421−1433

53: purification by flash chromatography over silica (hexane/diethyl ether 4/1). Yield: 55.0 mg (49%) using **Λ-1P**. FT-IR (ATR; ν, cm^{-1}): 3479, 2961, 1706, 1370, 1280, 1250, 1147, 1107, 1015. ^1H NMR (400 MHz, $CDCl_3$, 300 K; δ, ppm): 2.43 (d, J = 5.6 Hz, 1H), 2.0 (m, 1H), 1.95 (s, 3H), 1.9−1.8 (m, 4H), 1.6−1.2 (m, 6H), 1.54 (s, 3H), 1.17 (s, 3H), 1.15 (s, 3H), 1.02 (s, 3H). ^{13}C NMR (75 MHz, $CDCl_3$, 300 K; δ, ppm): 170.4, 85.8, 79.4, 57.3, 54.8, 53.7, 44.8, 41.2, 35.7, 33.5, 29.6, 27.9, 26.7, 25.8, 24.2, 22.7, 21.4; in agreement with those reported in the literature.[20,75] ESI-MS (m/z): 303.2 $[M + Na]^+$.

58: purification by flash chromatography over silica (dichloromethane). FT-IR (ATR; ν, cm^{-1}): 3419, 2962, 2933, 1778, 1372, 1219, 1148, 923. ^1H NMR (400 MHz, $CDCl_3$, 300 K; δ, ppm): 5.23−5.19 (m, 1H), 2.09 (ddd, J_1 = 2.7, J_2 = 4.6, J_3 = 12.7 Hz; 1H) 1.91−1.82 (m, 1H), 1.72−1.66 (m, 1H), 1.62−1.46 (m, 5H), 1.28 (s, 3H), 0.94 (d, J = 7.0 Hz, 3H), 0.83 (d, J = 7.0 Hz, 3H). ^{13}C NMR (100 MHz, $CDCl_3$, 300 K; δ, ppm): 157, 114.6, 77.4, 71.1, 46.6, 43.8, 37.7, 31.3, 26.2, 20.6, 19.2, 16.3. HRMS (ESI-TOF, $[M + Na]^+$): m/z calcd for $C_{12}H_{19}F_3O_3Na$ 291.1178, found 291.1161.

59. Purification by flash chromatography over silica (dichloromethane). FT-IR (ATR; ν, cm^{-1}): 2965, 2937, 1780, 1717, 1372, 1220, 1157. ^1H NMR (400 MHz, $CDCl_3$, 300 K; δ, ppm): 5.25 (dt, J_1 = 4.4, J_2 = 10.8 Hz; 1H), 2.59 - 2.50 (m, 1H) 2.45−2.38 (m, 2H), 2.18 (dt, J_3 = 1.1, J_4 = 13.7 Hz; 1H), 2.12 - 2.02 (m, 2H), 1.95 - 1.88 (m, 1H), 1.07 (d, J = 1.07 Hz, 3H), 0.91 (d, J = 7.0 Hz, 3H), 0.85 (d, J = 6.8 Hz, 3H). ^{13}C NMR (100 MHz, $CDCl_3$, 300 K; δ, ppm): 209.6, 157.2, 114.4, 76.0, 47.3, 41.7, 38.2, 38.0, 26.5, 20.1, 15.5, 14.0. HRMS (ESI-TOF, $[M + Na]^+$): m/z calcs for $C_{12}H_{17}F_3O_3Na$ 289.1022, found 289.1045.

61: purification by flash chromatography over silica (hexane/ethyl acetate 90/10). Yield: 44.8 mg (52%) using **Λ-2P**. FT-IR (ATR; ν, cm^{-1}): 3423, 2960, 2938, 2872, 1739, 1717, 1370, 1257, 1023, 790. ^1H NMR (400 MHz, $CDCl_3$, 300 K; δ, ppm): 4.82 (td, J = 9.8, 4.3 Hz, 1H), 2.05 (s, 3H), 1.98 (ddd, J = 12.3, 4.3, 2.0, 1H), 1.85−1.77 (m, 1H), 1.73−1.66 (m, 2H), 1.55−1.37 (m, 3H), 1.26 (s, 3H), 1.23−1.14 (m, 1H), 0.93 (d, J = 6.7 Hz, 3H), 0.81 (d, J = 6.9 Hz, 3H). ^{13}C NMR (100 MHz, $CDCl_3$, 300 K; δ, ppm): 170.4, 72.0, 70.8, 46.5, 44.5, 38.5, 26.8, 26.0, 21.3, 20.8, 20.2, 17.0. HRMS (ESI-TOF, $[M + Na]^+$): m/z calcd for $C_{12}H_{22}O_3Na$ 237.1461, found 237.1466.

62: purification by flash chromatography over silica (hexane/ethyl acetate 90/10). Yield: 9.1 mg (11%) using **Λ-2P**. FT-IR (ATR; ν, cm^{-1}): 2961, 2928, 2872, 1714, 1365, 1235, 1030, 803. ^1H NMR (400 MHz, $CDCl_3$, 300 K; δ, ppm): 5.23 (q, J = 3.6 Hz, 1H), 2.69−2.62 (m, 2H), 2.39 (dd, J = 14.2, 4.8 Hz, 1H), 2.12 (s, 3H), 1.92−1.88 (m, 1H), 1.74 (ddd, J = 14.7, 11.8, 3.2 Hz, 1H), 1.48−1.39 (m, 1H), 1.28−1.22 (m, 1H), 1.05 (d, J = 6.7 Hz, 3H), 0.96 (d, J = 6.8 Hz, 3H), 0.94 (d, J = 6.8 Hz, 3H). ^{13}C NMR (100 MHz, $CDCl_3$, 300 K; δ, ppm): 212.5, 170.4, 70.3, 48.0, 40.1, 39.1, 35.6, 28.6, 21.4, 20.3, 20.1, 14.4. HRMS (ESI-TOF, $[M + Na]^+$): m/z calcd for $C_{12}H_{20}O_3Na$ 235.1305, found 235.1309.

64: purification by flash chromatography over silica (hexane). Yield: 66.2 mg (65%) using **Δ-1P**. FT-IR (ATR; ν, cm^{-1}): 3310, 2960, 2937, 2871, 1720, 1167, 1153, 1127. ^1H NMR (400 MHz, $CDCl_3$, 300 K; δ, ppm): 4.81 (td, J = 9.3, 4.1 Hz, 1H), 1.98−1.92 (m, 1H), 1.87−1.77 (m, 1H), 1.75−1.64 (m, 2H), 1.55−1.39 (m, 3H), 1.28−1.22 (m, 1H), 1.25 (s, 3H), 1.19 (s, 9H), 0.94 (d, J = 6.9 Hz, 3H), 0.81 (d, J = 6.9 Hz, 3H). ^{13}C NMR (100 MHz, $CDCl_3$, 300 K; δ, ppm): 177.7, 71.9, 70.7, 46.3, 43.8, 38.8, 38.2, 27.2, 27.1, 26.0, 20.9, 19.9, 17.2. HRMS (ESI-TOF, $[M + Na]^+$): m/z calcd for $C_{15}H_{28}O_3Na$ 279.1931, found 279.1918.

65: purification by flash chromatography over silica (hexane). Yield: 9.4 mg (9%) using **Δ-1P**. FT-IR (ATR; ν, cm^{-1}): 2959, 2932, 2873, 1718, 1283, 1152, 1122. ^1H NMR (400 MHz, $CDCl_3$, 300 K; δ, ppm): 5.20 (dd, J = 7.1, 3.5 Hz, 1H), 2.70−2.58 (m, 2H), 2.41 (dd, J = 14.1, 4.4 Hz, 1H), 2.15−2.09 (m, 1H), 1.93−1.71 (m, 3H), 1.25 (s, 9H), 0.96 (d, J = 6.7, 3H), 0.93 (d, J = 7.0, 3H). ^{13}C NMR (100 MHz, $CDCl_3$, 300 K; δ, ppm): 212.4, 177.7, 69.9, 48.0, 40.2, 39.2, 35.5, 28.7, 27.1, 27.0, 20.3, 20.2,14.5. HRMS (ESI-TOF, $[M + Na]^+$): m/z calcd for $C_{15}H_{26}O_3Na$ 277.1774, found 277.1762.

67: purification by flash chromatography over silica (hexane). Yield: 20.6 mg (24%) using **Λ-1P**. FT-IR (ATR; ν, cm^{-1}): 3420, 2928, 1737, 1216, 1132. ^1H NMR (400 MHz, $CDCl_3$, 300 K; δ, ppm): 5.39−5.35 (m, 1H), 2.07 (s, 3H), 2.00−1.92 (m, 1H) 1.86−1.79 (m, 1H), 1.77−1.57 (m, 3H), 1.42−1.37 (m, 1H), 1.20 (s, 3H), 1.16 (s, 3H), 1.11−0.91 (m, 2H), 0.87 (d, J = 6.7 Hz, 3H). ^{13}C NMR (100 MHz, $CDCl_3$, 300 K; δ, ppm): 170.7, 71.9, 71.2, 49.9, 39.4, 34.7, 28.7, 27.6, 26.6, 22.1, 22.0, 21.6. HRMS (ESI-TOF, $[M + Na]^+$): m/z calcd for $C_{12}H_{22}O_3Na$ 237.1461, found 237.1458.

68: purification by flash chromatography over silica (hexane). Yield: 15.3 mg (18%) using **Λ-1P**. FT-IR (ATR; ν, cm^{-1}): 2970, 2930, 1733, 1708, 1371, 1242, 1028. ^1H NMR (400 MHz, $CDCl_3$, 300 K; δ, ppm): 5.34−3.32 (m, 1H), 2.70−2.59 (m, 1H), 2.54−2.40 (m, 2H), 2.38−2.30 (m, 1H), 2.13 (s, 3H), 1.69−1.46 (m, 3H), 1.01 (d, J = 6.4 Hz, 3H), 0.93 (d, J = 6.4 Hz, 3H), 0.89 (d, J = 6.5 Hz, 3H). ^{13}C NMR (100 MHz, $CDCl_3$, 300 K; δ, ppm): 212.0, 170.4, 69.1, 49.0, 41.3, 38.9, 38.9, 29.6, 21.2, 20.6, 20.4, 13.7. HRMS (ESI-TOF, $[M + Na]^+$): m/z calcd for $C_{12}H_{20}O_3Na$ 235.1305, found 235.1303.

73: purification by flash chromatography over silica (dichloromethane). Yield: 31.1 mg (29%) using **Λ-1P**. FT-IR (ATR; ν, cm^{-1}): 3281, 2934, 2871, 1772, 1365, 1325, 1216, 1131, 919. ^1H NMR (400 MHz, $CDCl_3$, 300 K; δ, ppm): 5.62−5.59 (m, 1H), 2.08−2.02 (m, 1H) 1.90−1.84 (m, 1H), 1.79−1.61 (m, 3H), 1.53−1.48 (m, 1H), 1.22 (s, 3H), 1.19 (s, 3H), 1.07−0.90 (m, 2H), 0.90 (d, J = 6.6 Hz, 3H). ^{13}C NMR (100 MHz, $CDCl_3$, 300 K; δ, ppm): 156.8, 114.6, 76.1, 71.9, 50.3, 38.9, 34.5, 28.9, 27.6, 26.4, 21.9, 21.8. HRMS (ESI-TOF, $[M + Na]^+$): m/z calcd for $C_{12}H_{19}F_3O_3Na$ 291.1178, found 291.1157.

74: purification by flash chromatography over silica (dichloromethane). Yield: 6.4 mg (6%) using **Λ-1P**. FT-IR (ATR; ν, cm^{-1}): 2970, 2936, 2877, 1780, 1715, 1374, 1341, 1218, 1149, 893. ^1H NMR (400 MHz, $CDCl_3$, 300 K; δ, ppm): 5.54 (m, 1H), 2.68−2.54 (m, 2H), 2.49−2.39 (m, 2H), 1.71−1.58 (m, 3H), 1.05 (d, J = 6.5 Hz, 3H), 0.95 (d, J = 6.4 Hz, 3H), 0.93 (d, J = 6.5 Hz, 3H). ^{13}C NMR (100 MHz, $CDCl_3$, 300 K; δ, ppm): 210.4, 157.0, 114.6, 74.5, 48.8, 40.9, 38.6, 38.2, 29.5, 20.5, 20.3, 13.7. HRMS (ESI-TOF, $[M + Na]^+$): m/z calcd for $C_{12}H_{17}F_3O_3Na$ 289.1022, found 289.1037.

*Millimole Scale Reactions. Substrate: **51** and **75**.* A round-bottom flask was charged with catalyst (21 μmol, 3 mol %), alkane (0.7 mmol, 1 equiv), CH_3CN (14 mL), and a magnetic stir bar. A 1.74 M CH_3CO_2H solution in CH_3CN was added (0.6 mL, 1.05 mmol, 150 mol %), the mixture was placed in an ice bath or an CH_3CN/N_2 bath, and the contents were stirred. The necessary amount of a 1.5 M (X equiv, see Table 2) H_2O_2 solution (diluted from a 35% H_2O_2 aqueous solution) was delivered by syringe pump over 17 min at 0 or −35 °C. After syringe pump addition, the solution was stirred for 10 min at 0 or −35 °C. Solvent was removed under reduced pressure, and the resulting residue was purified by flash chromatography on silica gel. If necessary, the recovered starting material was submitted to a second oxidation using the aforementioned procedure and employing proportional amounts of each reactant, so that the proportions stay the same. Workup was identical with the former procedure. If necessary, a third oxidation can be done in the same way.

76: purification of products by flash chromatography over silica (hexane/diethyl ether from 30/1 to 1/1). Yield: 86.1 mg (48%) using **Λ-1P**. FT-IR (ATR; ν, cm^{-1}): 3340, 2948, 1717, 1478, 1283, 1140, 928, 897. ^1H NMR (400 MHz, $CDCl_3$, 300 K; δ, ppm): 5.36−5.35 (m, 1H), 1.95−1.89 (m, 1H), 1.87−1.81 (m, 1H), 1.78−1.60 (m, 3H), 1.44−39 (m, 1H), 1.22 (s, 9H), 1.20 (s, 3H), 1.16 (s, 3H), 1.11−0.91 (m, 2H), 0.88 (d, J = 6.6 Hz, 3H). ^{13}C NMR (100 MHz, $CDCl_3$, 300 K; δ, ppm): 178.0, 71.9, 71.2, 49.9, 39.5, 39.0, 34.8, 28.8, 27.6, 27.2, 26.8, 22.2, 22.1. HRMS (ESI-TOF, $[M + Na]^+$): m/z calcd for $C_{15}H_{28}O_3Na$ 279.1931, found 279.1909.

77: purification of products by flash chromatography over silica (hexane/diethyl ether from 30/1 to 1/1). Yield: 51.6 mg (29%) using **Δ-1P**. FT-IR (ATR; ν, cm^{-1}): 2963, 2930, 2871, 1708, 1476, 1285, 1156, 1127. ^1H NMR (400 MHz, $CDCl_3$, 300 K; δ, ppm): 5.27 (m, 1H), 2.62−2.49 (m, 2H), 2.44−2.30 (m, 2H), 1.60−1.50 (m, 3H), 1.25 (s, 9H), 1.01 (d, J = 6.6 Hz, 3H), 0.92 (d, J = 6.9 Hz, 3H), 0.88 (d, J = 6.5 Hz, 3H). ^{13}C NMR (100 MHz, $CDCl_3$, 300 K; δ, ppm): 212.0, 177.7, 68.7, 49.3, 41.7, 39.3, 38.9, 38.8, 29.8, 27.2, 20.6, 20.5, 13.9. HRMS (ESI-TOF, $[M + Na]^+$): m/z calcd for $C_{15}H_{26}O_3Na$ 277.1774, found 277.1758.

dx.doi.org/10.1021/jo302196q | J. Org. Chem. 2013, 78, 1421−1433

78: product purification by flash chromatography over silica (product was eluted with a 1/1 hexane/diethyl ether mixture). Yield: 66.6 mg (36%) using **Λ-2P**, at −35 °C. FT-IR (ATR; ν, cm^{-1}): 3014, 2952, 2924, 2854, 1772, 1695, 1182, 1020, 921. ^1H NMR (400 MHz, $CDCl_3$, 300 K; δ, ppm): 2.97 (dd, J = 17.0, 6.5 Hz, 1H), 2.68 (ddd, J = 15.7, 9.2, 5.1 Hz, 1H), 2.54 (dd, J = 17.0, 14.2 Hz, 1H), 2.29 (ddd, J = 15.7, 8.4, 5.0 Hz, 1H), 2.15 (dd, J = 14.2, 6.6 Hz, 1H), 2.09 (dd, J = 11.1, 2.7 Hz, 1H), 1.93−1.88 (m, 1H), 1.87−1.81 (m, 1H), 1.69 (dd, J = 9.2, 5.0 Hz, 1H), 1.66−1.62 (m, 1H), 1.58 (dd, J = 13.2, 3.1 Hz, 1H), 1.54−1.49 (m, 1H), 1.35 (s, 3H), 1.19 (s, 3H), 1.06 (s, 3H), 1.02 (s, 3H).). ^{13}C NMR (100 MHz, $CDCl_3$, 300 K; δ, ppm): 214.2, 176.8, 85.7, 53.8, 52.0, 49.6, 39.1, 37.7, 34.5, 32.4, 31.3, 30.8, 23.2, 21.7, 21.1, 14.4; in agreement with those reported in the literature.[70] GC-MS (m/z): 282.2 $[M + NH_4]^+$.

79: product purification by flash chromatography over silica (product was eluted with a 1/2 hexane/diethyl ether mixture).Yield: 74.0 mg (40%) using **Δ-1P**. FT-IR (ATR; ν, cm^{-1}): 2940, 1781, 1701, 1186, 1112, 1034, 915. ^1H NMR (400 MHz, $CDCl_3$, 300 K; δ, ppm): 2.48−2.41 (m, 1H), 2.32−2.11 (m, 7H), 2.06−1.98 (m, 1H), 1.85−1.44 (m, 3H), 1.35 (s, 3H), 1.09 (s, 3H), 0.93 (s, 6H). ^{13}C NMR (100 MHz, $CDCl_3$, 300 K; δ, ppm): 209.3, 175.6, 85.6, 58.2, 56.6, 55.6, 54.9, 40.3, 38.6, 38.0, 33.3, 28.6, 22.6, 21.1, 20.7, 16.2; in agreement with those reported in the literature.[52] GC-MS (m/z): 282.2 $[M + NH_4]^+$.

79OH: product purification by flash chromatography over silica (product was eluted with a 1/10 hexane/diethyl ether mixture). Yield: 8.4 mg (4.5%) using **Λ-2P**. FT-IR (ATR; ν, cm^{-1}): 3455, 3024, 2970, 2925, 1739, 1436, 1365, 1217. ^1H NMR (400 MHz, $CDCl_3$, 300 K; δ, ppm): 4.04−3.96 (m, 1H), 2.45 (dd, J = 16.2, 14.7 Hz, 1H), 2.27 (dd, J = 16.2, 6.5 Hz, 1H), 2.10 (dt, J = 11.8, 3.3 Hz, 1H), 2.01 (dd, J = 14.8, 6.5 Hz, 1H), 1.93−1.89 (m, 1H), 1.87−1.84 (m, 1H), 1.83−1.81 (m, 1H), 1.74−1.67 (td, J = 12.1, 3.5 Hz, 1H), 1.58−1.52 (m, 1H), 1.43−1.40 (m, 1H), 1.39−1.35 (m, 1H), 1.34 (d, J = 0.92 Hz, 3H), 1.15−1.10 (m, 1H), 0.97 (s, 3H), 0.96 (s, 3H), 0.89 (s, 3H). ^{13}C NMR (100 MHz, $CDCl_3$, 300 K; δ, ppm): 176.0, 86.0, 64.4, 58.9, 56.2, 51.5, 48.4, 38.5, 37.4, 34.8, 33.2, 28.7, 21.8, 21.6, 20.2, 16.1; in agreement with those reported in the literature.[76] GC-MS (m/z): 284.2 $[M + NH_4]^+$.

80: product purification by flash chromatography over silica (product was eluted with a 1/1.5 hexane/diethyl ether mixture). Yield: 62.9 mg (34%) using **Λ-2P**, at 0 °C. FT-IR (ATR; ν, cm^{-1}): 2914, 1773, 1695, 1392, 1228, 1193, 1170, 1034, 962. ^1H NMR (400 MHz, $CDCl_3$, 300 K; δ, ppm): 2.63−2.40 (m, 3H), 2.29 (ddd, J = 16.2, 6.5, 0.4 Hz, 1H), 2.14 (dt, J = 11.6, 3.0 Hz, 1H), 2.01 (dd, J = 14.7, 6.5 Hz, 1H), 1.87.1.82 (m, 1H), 1.78−1.70 (m, 2H), 1.65−1.53 (m, 3H), 1.39 (s, 3H), 1.13 (s, 3H), 1.06 (s, 3H), 1.03 (s, 3H). ^{13}C NMR (100 MHz, $CDCl_3$, 300 K; δ, ppm): 215.5, 175.9, 85.6, 58.1, 54.3, 47.4, 37.73, 37.68, 35.3, 33.4, 28.6, 26.6, 21.4, 21.1, 20.7, 14.5; in agreement with those reported in the literature.[52] GC-MS (m/z): 282.2 $[M + NH_4]^+$.

■ ASSOCIATED CONTENT

Supporting Information

Text, figures, tables, and CIF files giving full oxidation catalysis results, NMR spectra, crystallographic data. This material is available free of charge via the Internet at http://pubs.acs.org.

■ AUTHOR INFORMATION

Corresponding Author

*E-mail: Miquel.costas@udg.edu.

Notes

The authors declare no competing financial interest.

†Authors contributed equally to this work.

■ ACKNOWLEDGMENTS

We thank the European Research Foundation for Starting Grant Project ERC-2009-StG-239910, MICINN for project CTQ2009-08464 and a Ph.D. grant (I.P.), and the Generalitat de Catalunya for a Ph.D. grant (M. Canta). X.R. thanks financial support from INNPLANTA project INP-2011-0059-PCT-420000-ACT1. M.C. and X.R. thank ICREA Academia Awards.

■ REFERENCES

(1) Chen, K.; Baran, P. S. *Nature* **2009**, *459*, 824.
(2) Maimone, T. J.; Baran, P. S. *Nat. Chem. Biol* **2007**, *3*, 396.
(3) Hanson, J. R. *Nat. Prod. Rep.* **2010**, *27*, 887.
(4) Zhang, K.; Shafer, B. M.; Matthew, D.; Demars, I.; Stern, H. A.; Fasan, R. *J. Am. Chem. Soc.* **2012**, *134*, 18695.
(5) Mendoza, A.; Ishihara, Y.; Baran, P. S. *Nat. Chem.* **2012**, *4*, 21.
(6) Wender, P. A.; Hilinski, M. K.; Mayweg, A. V. W. *Org. Lett.* **2005**, *7*, 79.
(7) Newhouse, T.; Baran, P. S. *Angew. Chem., Int. Ed.* **2011**, *50*, 3362.
(8) Gutekunst, W. R.; Baran, P. S. *Chem. Soc. Rev.* **2011**, *40*, 1976.
(9) McMurray, L.; O'Hara, F.; Gaunt, M. J. *Chem. Soc. Rev.* **2011**, *40*, 1885.
(10) Zhou, M.; Crabtree, R. H. *Chem. Soc. Rev.* **2011**, *40*, 1875.
(11) Lu, H.; Zhang, P. *Chem. Soc. Rev.* **2011**, *40*, 1899.
(12) Company, A.; Gomez, L.; Costas, M. In *Iron-Containing Enzymes, Versatile Catalysts of Hydroxylation Reactions in Nature*; De Visser, S. P., Kumar, D., Eds.; Royal Society of Chemistry: Cambridge, U.K., 2011.
(13) White, M. C. *Science* **2012**, *335*, 807.
(14) Shul'pin, G. B. *Org. Biomol. Chem.* **2010**, *8*, 4217.
(15) Lee, S.; Fuchs, P. L. *J. Am. Chem. Soc.* **2002**, *124*, 13978.
(16) Brodsky, B. H.; Du Bois, J. *J. Am. Chem. Soc.* **2005**, *127*, 15391.
(17) Curci, R.; D'Accolti, L.; Fusco, C. *Acc. Chem. Res.* **2006**, *39*, 1.
(18) Litvinas, N. D.; Brodsky, B. H.; Du Bois, J. *Angew. Chem., Int. Ed.* **2009**, 4513.
(19) McNeill, E.; Bois, J. D. *J. Am. Chem. Soc.* **2010**, *132*, 10202.
(20) Tenaglia, A.; Terranova, E.; Waegell, B. *J. Org. Chem.* **1992**, *57*, 5523.
(21) McNeill, E.; Bois, J. D. *Chem. Sci.* **2012**, *3*, 1810.
(22) Barton, D. H. R.; Doller, D. *Acc. Chem. Res.* **1992**, *25*, 504.
(23) Barton, D. H. R.; Li, T.; Mackinnon, J. *Chem. Commun.* **1997**, 557.
(24) Kamata, K.; Yonehara, K.; Nakagawa, Y.; Uehara, K.; Mizuno, N. *Nat. Chem.* **2010**, *2*, 478.
(25) Zhao, Y.; Yim, W.-L.; Tan, C. K.; Yeung, Y.-Y. *Org. Lett.* **2011**, *13*, 4308.
(26) Larsen, A. T.; May, E. M.; Auclair, K. *J. Am. Chem. Soc.* **2011**, *133*, 7853.
(27) Moreira, R. F.; Wehn, P. M.; Sames, D. *Angew. Chem., Int. Ed.* **2000**, *39*, 1618.
(28) Desai, L. V.; Hull, K. L.; Sanford, M. S. *J. Am. Chem. Soc.* **2004**, *126*, 9542.
(29) Chen, K.; Richter, J. M.; Baran, P. S. *J. Am. Chem. Soc.* **2008**, *130*, 7247.
(30) Kasuya, S.; Kamijo, S.; Inoue, M. *Org. Lett.* **2009**, *11*, 3630.
(31) Simmons, E. M.; Hartwig, J. F. *Nature* **2011**, *483*, 70.
(32) Giri, R.; Liang, J.; Lei, J.-G.; Li, J.-J.; Wang, D.-H.; Chen, X.; Naggar, I. C.; Guo, C; Foxman, B. M.; Yu, J.-Q. *Angew. Chem., Int. Ed.* **2005**, *44*, 7420.
(33) Das, S.; Incarvito, C. D.; Crabtree, R. H.; Brudvig, G. W. *Science* **2006**, *312*, 1941.
(34) Bigi, M. A.; Reed, S. A.; White, M. C. *J. Am. Chem. Soc.* **2012**, *134*, 9721.
(35) Zhang, S.-Y.; He, G.; Zhao, Y.; Wright, K.; Nack, W. A.; Chen, G. *J. Am. Chem. Soc.* **2012**, *134*, 7313.
(36) Wang, Y.-F.; Chen, H.; Zhu, X.; Chiba, S. *J. Am. Chem. Soc.* **2012**, *134*, 11980.
(37) Sun, C.-L.; Li, B.-J.; Shi, Z.-J. *Chem. Rev.* **2011**, *111*, 1293.
(38) Que, L.; Tolman, W. B. *Nature* **2008**, *455*, 333.
(39) Kovaleva, E. G.; Lipscomb, J. D. *Nat. Chem. Biol.* **2008**, *4*, 186.
(40) Bruijnincx, P. C. A.; Koten, G. v.; Gebbink, R. J. M. K. *Chem. Soc. Rev.* **2008**, *12*, 2716.

(41) Mukherjee, A.; Martinho, M.; Bominaar, E. L.; Munck, E.; Que, L. *Angew. Chem., Int. Ed.* **2009**, *48*, 1780.
(42) Comba, P.; Maurer, M.; Vadivelu, P. *Inorg. Chem.* **2009**, *48*, 10389.
(43) Yoon, J.; Wilson, S. A.; Jang, Y. K.; Seo, M. S.; Nehru, K.; Hedman, B.; Hodgson, K. O.; Bill, E.; Solomon, E. I.; Nam, W. *Angew. Chem., Int. Ed.* **2009**, *48*, 1257.
(44) Liu, P.; Liu, Y.; Wong, E. L.-M.; Xiang, S.; Che, C.-M. *Chem. Sci.* **2011**, *2*, 2187.
(45) Chen, K.; Que, L., Jr. *J. Am. Chem. Soc.* **2001**, *123*, 6327.
(46) Enthaler, S.; Junge, K.; Beller, M. *Angew. Chem., Int. Ed.* **2008**, *47*, 3317.
(47) Correa, A.; Mancheno, O. G.; Bolm, C. *Chem. Soc. Rev.* **2008**, *37*, 1108.
(48) Costas, M.; Chen, K.; Que, L., Jr. *Coord. Chem. Rev.* **2000**, *200*–*202*, 517.
(49) Chen, M. S.; White, M. C. *Science* **2007**, *318*, 783.
(50) Company, A.; Gómez, L.; Fontrodona, X.; Ribas, X.; Costas, M. *Chem. Eur. J.* **2008**, *14*, 5727.
(51) Gomez, L.; Garcia-Bosch, I.; Company, A.; Benet-Buchholz, J.; Polo, A.; Sala, X.; Ribas, X.; Costas, M. *Angew. Chem., Int. Ed.* **2009**, *48*, 5720.
(52) Chen, M. S.; White, M. C. *Science* **2010**, *327*, 566.
(53) He, Y.; Gorden, J. D.; Goldsmith, C. R. *Inorg. Chem.* **2011**, *50*, 12651.
(54) Hitomi, Y.; Arakawa, K.; Funabiki, T.; Kodera, M. *Angew. Chem., Int. Ed.* **2012**, *51*, 3448.
(55) For a recent related manganese-based system see Ottenbacher, R. V.; Samsonenko, D. G.; Talsi, E. P.; Bryliakov, K. P. *Org. Lett.* **2012**, *14*, 4310.
(56) Knof, U.; von Zelewsky, A. *Angew. Chem., Int. Ed.* **1999**, *38*, 302.
(57) Costas, M.; Tipton, A. K.; Chen, K.; Jo, D.-H.; Que, L., Jr. *J. Am. Chem. Soc.* **2001**, *123*, 6722.
(58) Suzuki, K.; Oldenburg, P. D.; Que, L., Jr. *Angew. Chem., Int. Ed.* **2008**, *47*, 1887.
(59) Costas, M.; Que, L., Jr. *Angew. Chem., Int. Ed.* **2002**, *12*, 2179.
(60) Barton, D. H. R.; Bévière, S. D.; Chavasiri, W.; Csuhai, E.; Doller, D.; Liu, W.-G. *J. Am. Chem. Soc.* **1992**, *114*, 2147.
(61) Shul'pin, G. B.; Kozlov, Y. N.; Shul'pina, L. S.; Kudinov, A. R.; Mandelli, D. *Inorg. Chem.* **2009**, *48*, 10480.
(62) Shul'pin, G. B.; Kozlov, Y. N.; Shul'pina, L. S.; Petrovskiy, P. V. *Appl. Organomet. Chem.* **2010**, *24*, 464.
(63) Shul'pin, G. B.; Suss-Fink, G.; Smith, J. R. L. *Tetrahedron* **1999**, *55*, 5345.
(64) Chen, K.; Eschenmoser, A.; Baran, P. S. *Angew. Chem., Int. Ed.* **2009**, *48*, 9705.
(65) Cook, B. R.; Reinert, T. J.; Suslick, K. S. *J. Am. Chem. Soc.* **1986**, *108*, 7281.
(66) Battioni, P.; Renaud, J. P.; Bartoli, J. F.; Reina-Artiles, M.; Fort, M.; Mansuy, D. *J. Am. Chem. Soc.* **1988**, *110*, 8462.
(67) Barton, D. H. R.; Beloeil, J.-C.; Billion, A.; Boivin, J.; Lallemand, J.-Y.; Lelandais, P.; Mergui, S. *Helv. Chim. Acta* **1987**, *70*, 2187.
(68) Härtner, J.; Reinscheid, U. M. *J. Mol. Struct.* **2008**, 872.
(69) Chapman, N. B.; Parker, R. E.; Smith, P. J. A. *J. Chem. Soc.* **1960**, 3634.
(70) Cano, A.; Ramírez-Apan, M. T.; Delgado, G. *J. Braz. Chem. Soc.* **2011**, *22*, 1177.
(71) Liu, W.; Groves, J. T. *J. Am. Chem. Soc.* **2010**, *132*, 12847.
(72) Bartoli, J. F.; Brigaud, O.; Battioni, P.; Mansuy, D. *J. Chem. Soc., Chem. Commun.* **1991**, 440.
(73) Wang, C.; Shalyaev, K. V.; Bonchio, M.; Carofiglio, T.; Groves, J. T. *Inorg. Chem.* **2006**, *45*, 4769.
(74) Groves, J. T.; Viski, P. *J. Am. Chem. Soc.* **1989**, *111*, 8537.
(75) Shiao, M.-J.; Lin, J. L.; Kuo, Y.-H.; Shih, K.-S. *Tetrahedron Lett.* **1986**, *27*, 4059.
(76) Choudhary, M. I.; Musharraf, S. G.; Sami, A.; Atta-ur-Rahman. *Helv. Chim. Acta* **2004**, *87*, 2685.